Bus Bike Rack Lifter

By

Dylan Baker-Flynn

Cole Flegel

Approved:

Professor Eben C. Cobb, Major Advisor

Bus Bike Rack Lifter MQP

A Major Qualifying Project Report

Submitted to the Faculty of the

WORCESTER POLYTECHNIC INSTITUTE

In partial fulfillment of the requirements for the Degree of Bachelor of Science

by

Dylan Baker-Flynn

Cole Flegel

Date:

18 May 2020

Report Submitted to:

Professor Eben Cobb

Worcester Polytechnic Institute

Abstract

The use of public transportation has risen significantly over the past two decades, as well as the use of bicycles by commuters to travel to and from stops. However, the limited bike storage on city buses does not always account for the number of riders. This purpose of this project is to initiate the development of a bus bike rack that not only stores more bicycles but also solves other issues with current bus bike racks, such as storing the bikes out of the bus driver's view to the front and keeping the bus at its standard length. The device allows four standard-wheelbase road and mountain bikes to be loaded onto the rack at the front of city buses. Once bikes are loaded on the rack, the rack lifts to the top of the bus. This project not only provides a new method of storing bicycles on city buses, but it also acts as a first step toward encouraging further use of both bicycles and public transportation for daily commute.

Acknowledgments

The design team would like to thank their advisor, Prof. Eben C. Cobb, for his guidance and constant advice and encouragement over the course of the academic year. The team would like to thank the staff of the Washburn Shops and the Foisie Innovation Studio Makerspace for providing a location and guidance in manufacturing the half-scale model of the project. We would also like to thank fellow students Maricella Ramirez and Jianqing Zhu for help with the mechatronic analysis of the four-bar mechanism. A special thank you also goes out to Peter Hefti, Patricia Howe, and Adriana Hera for additional help and guidance with specific elements of the project. Lastly, the team would like to thank all of the professors that have prepared them for this project and their friends and family for endless support and encouragement throughout the project.

Table of Contents

List of Figures

Chapter 1. Introduction

Some commuters that use municipal buses like to bike to or from the stops rather than walk. Some current buses utilize fold-down racks at the front of the buses; however, they can only hold a maximum of two or three bikes due to restrictions to the maximum length of buses when in motion [15]. This system can be problematic if more bicycle riders would like to store their bikes on the bus as they ride. If there is no longer an available space on the rack, the rider must wait for another bus with bike rack space, leave their bike at the stop and board the bus, or find an alternate method of commuting the rest of the way to their destination. As most commuters do not tend to account for these kinds of large-scale issues with their commute, this issue of limited rack space can be detrimental.

1.1. Expected Outcome

The design team set out to design a new system that allows more bicycles to be stored on the bus in order to encourage use of both bicycles and public transportation through ease of use. The design team researched the necessary parameters involved with adding a rack to standard city buses and regulations of their application to guide our design and ensure that what the design team designed would be both legal and feasible for use. A new rack would be designed using the researched parameters to improve the space restrictions, as well as other issues that come about in the research. Using analyses, such as the virtual work method of kinematics, the team would then be able to analyze the design and determine values such as necessary torque output required by an electric motor. Using the results from our analyses, the team would then constructed a prototype as a proof of concept, followed by testing and physical analysis to assess whether the device could meet the functional requirements. Once our design is complete, success would be determined and recommendations for further design work or operation of the device would be given.

1.2. Client Statement

Design a new rack system that allows more bikes to be stored on the bus. The rack should be manufactured for use with existing city buses to make it desirable for purchase. The goal is to design a rack that can be installed and removed without modifying the bus.

Chapter 2. Background

To better understand the issues associated with the current style of bus bike racks, the team conducted research into how bus bike racks are currently designed, how they perform, and issues that other research groups have discovered. The team also looked into the parameters that our design must follow, including laws governing city buses and their attachments, the measurements of commonly used commuter bicycle styles, and the average size and associated strength of commuters for operation of the rack. From this collected information, functional specifications were determined to guide our design.

2.1. Current Practices

Although there are different manufacturers and styles, almost all commercially produced racks have the same general design. As seen in Figure 1, bikes are currently stored sideways on city buses. The rack folds down from the front bumper of the bus and a spring-loaded arm clamps the front tire down onto the rack secure the bikes. Most racks hold two or three bicycles with a standard wheelbase of a mountain bike or road bike.

Figure 1: Current Rack System

As rear-mounted racks allow for a greater chance of the bicycles being stolen, damaged, or forgotten by riders, racks are mounted on the front of city buses [8]. Mounting racks on the front also negates the need to remove the rack to access rear panels for maintenance.

2.2. Issues with Current Practices

While the current design works in many circumstances, there are still a lot of limitations and concerns with some parameters that can affect the operation of the rack and bus in general. All current racks on buses are add-on units designed for a variety of bus brands and models and therefore are not always able to account for ideal operation of either the bus or rack.

In October 1997, the ACT Department of Urban Services performed an investigation into the issues associated with the engineering and safety of bike racks in use on the front of transit buses [1]. These concerns presented can offer additional recommendations on parameters the design team should consider with our design. Their concerns included:

1. The safety of pedestrians:
    a. Can the rack or the attached bicycles cause a hazard to pedestrians?
2. Maneuverability of the bus:
    a. Will the extra length at the front of the bus restrict the bus's ability to turn or change lanes (enter or exit the bus stops)?
    b. Will the limited ground clearance limit the bus's ability to clear obstacles?
3. Road space at bus stops:
    a. Will the extra length of the buses cause an issue with space at bus stops, especially with limiting the number of buses that can be at a bus stop at one time?
4. Driver visibility:
    a. Will the rack or attached bikes limit the visibility of the driver?
5. Headlight visibility:
    a. Will the rack or attached bikes reduce the effectiveness of the headlights of the bus?

6. Additional driver responsibilities:
    a. Will the additional responsibilities of ensuring proper loading and unloading of bikes place too much pressure on the driver?
    b. Will the driver be required to leave the bus to help load and unload if needed?
7. Effect of easier bike transit use:
    a. Will improved bike racks encourage more bike riding, which will require more road safety legislation or construction of additional bike lanes?
    b. Will this trend continue to propagate and cause additional changes or cost?
8. Additional concerns:
    a. Will the rack and its mounting have adequate structural integrity and longevity for daily use?
    b. Will the rack influence or inhibit the cleaning and maintenance of the bus?
    c. Will the rack damage the bus or bikes?

2.3. Legal Parameters

To determine why the current bicycle attachment system has the functional specifications that it currently has and to determine what specifications the design team must employ for our design, the design team looked into the state and national regulations for buses and their attachments. According to California law, it is illegal for any attachment to a city bus to increase the total bus length to over 48.5 feet [2]. This is why commercial bus bike racks fit two or three bikes as any more than that would exceed the limit. Restrictions to the width of buses with side-mounted attachments is a federal limitation and limits the width to under 8.5 feet. However, states may grant special use permits to vehicles that exceed the limitation [15]. As the standard lane width in the United States is 12 feet, adding any significant racks to the sides of the bus would not be advisable as the buses may not fit on some streets, regardless of the legality. The design team have also chosen to attach the rack lifter to the top of the front of the bus, as the top of the bus is the only location that can store bikes while remaining in the size restrictions and the front of the bus is the ideal location for riders to mount bikes to ensure proper attachment to the rack.

2.4. Bicycle Parameters

The current style of bus bike rack accounts for the general size of road bikes and mountain bikes. These bikes have average wheelbases of 38.84 in. [9] and 46.73 in. [14], respectively. Road bikes also weigh 18 pounds, on average, whereas mountain bikes generally fall between 21-29 pounds, based on the specific characteristics and features of the bike. Considering other types of bikes, cruiser and touring style bikes are generally between 35-40 pounds, recumbent bikes weigh an average of 23 pounds, and smaller kids bikes a sturdy 24 pounds [11]. Because of the significant differences between the different styles of bikes, our bike rack will focus on being compatible with road and mountain bikes as they are the most common bikes.

2.5. Human Parameters

As the design team plan to have the new bike rack system manually operated by just the rider, the design team had to determine the physical limitations of the average human. It is reasonable to assume that passengers would not want to raise their arms above the height of their shoulders and increase the equivalent weight of the bike that they are lifting. According to a North Carolina State University study, the average shoulder height of an adult male is 56.79 inches; while the average height of an adult female's shoulder is 52.50 inches [6]. Most riders will lift their bikes near the standover height, which is, on average, 30 inches from the ground when standing. This requires riders to lift the bikes onto the rack a maximum of around two feet, on average. As a result, the design team should design our rack so that the lower "loading" position will require riders to lift bikes less than 22.50 inches to load.

The next human parameter that we had to consider is the weight of the device and the strength needed to operate it manually. We began by researching existing designs for racks and plan to base our weight limit upon that. Sportworks transit bike racks, used by over 500 transit agencies throughout North America, are limited to less than 30 pounds without bikes attached [13]. This allows for minimal weight held by the front of the bus's structure as well as easy operation by an average rider when folding the rack down or back up at the front of the bus. As the strength of the average bike rider can vary immensely, it is essential that we limit the effective weight of our device to make sure it can be operated manually, if needed.

2.6. Functional Specifications

The design team designated specifications pertaining to the function of the rack to design our new bus bike rack. In order to not keep the bus at the stop for too long and get off-schedule, the design team set the requirement that it must take under 15 seconds for riders to lower and lift the rack, in addition to 30 seconds to mount the bike securely on the rack. The design team are also requiring that the bus with the rack lowered must still fit in the space allotted to a standard bus stop. As the most common bus length is 40 feet [3] and the standard platform is 90-100 feet long (including lead-in and lead-out) [5], we decided that the rack must extend less than 5 feet in front of the bus [12] to accommodate for 2 buses parked within the platform area. This will be more difficult as the design team must have a longer rack to accommodate more bikes. Even now, the racks can sometimes limit the fit of buses in the designated locations. The design team have decided that being able to fit in the current space is vital to the use of the municipal bus system as a whole. We do not have to worry about any length restrictions while the bus is in motion as the rack will be on top of the bus and will not change the length of the bus at all.

Assuming that the average rider has a shoulder height of 54.645 inches, the design team can design the rack to set its height when lowered to be at a standard, reasonable height. The design team have also set the weight of the rack itself to be under 30 pounds as that is what is standard for transit bike racks. The links that lift the rack should not add any more than 20 pounds for a total weight of the linkage system of 50 pounds. The design team expect that the new rack, with additional components necessary for operation, will exceed the weight limit. If this is so, the design team will add gas springs to the rack to assist in lifting and reduce the effective weight to below the set level. The design team have set that the rack should carry a maximum of four bicycles so that the total force applied by the coupler link does not exceed 50 lbf.

Using our knowledge of mechanisms and materials that the design team believe could work well for the design at hand, in conjunction with details of current bus bike racks, the design team have chosen to design the rack and lifter mechanism using aluminum bars as links that will lift the rack. The design team will use an electric motor to power the drive link to lift and lower the rack, as it will require far more torque than the average riders can apply themselves.

Chapter 3. Design Concepts

An ideal solution to the issue at hand would be to completely redesign a bus entirely and design for use with bikes to optimize use of both. However, this is not a reasonable option now since the need for bike storage on buses is not urgent enough to require a complete overhaul of the system and the relationship between bus and bicycle commuting. As the need for an improved method of allowing bicycle commuters to utilize the municipal bus system for parts of their commute is not great enough to warrant that level of funding and effort as of now, our design can help bridge the gap between no need for change and the complete overhaul. Our design allows for minimal change and modification for the bus and can be added to and removed from the bus easily. This makes costs for implementation low and requires very little effort for the city or bus company to add to their existing buses.

Prior to designing the rack, the team discussed a variety of ways that the design team could improve bus bike racks from the current practices. In addition to standard mechanical and mechatronic systems, the design team also explored a large variety of solutions. These solutions included utilizing an electromagnet attached to the exterior of the bus to attach bikes all around the bus magnetically, changing legislation to allow all bikes inside the bus, completely redesigning buses to focus on storing bikes over passengers, and even redesigning streets to allow for bike attachment on the sides of the bus. The design team then focused our efforts on designing a mechanical or mechatronic system that was simply an improvement upon the current system.

3.1. Design

Our current design consists of a pair of drag-link four-bar linkages that lift the same style of rack that is currently in use at the front of buses to a position on top of the front of the bus. The linkages attach at 2 points on each side of the bus and attach to a “cage” that is attached to the roof of the bus in order to keep from modifying the bus itself. To keep the bicycles attached to the rack and minimize the strength of the system that secures the bikes to the rack, the coupler link containing the rack itself remains horizontal for the entirety of the travel of the linkage and moves at a very small velocity.

3.2. Solving Issues

These concerns provide additional information on how the design team can improve the current system of bus bike racks. Not only will the design team solve the problem of the rack not holding enough bikes, the design team can also take into account factors such as safety and ease of use. The design team hope that changing the current rack design will further solve these issues rather than add to them.

As our suggested design places the rack and attached bicycles on the top of the bus while the bus is in motion, any sort of interaction between the rack or bicycles and any pedestrians will be limited to when the bus is at a stop and is being lifted or lowered or bikes are being attached or removed. Assuming proper operation and maintenance of the lifter, the rack should not be any less safe than the current style.

Having the rack on the top of the bus also improves the maneuverability of the bus over those with the standard bike rack, as it is now lower and can take tighter turns and enter bus stop lanes more easily. As the stops generally include extra length for entry and exit, there will be sufficient room for lowering the rack for bike attachment and removal while at the stop. This should be true for stops designed for both singular and multiple buses, but available space may vary, as bus stop specifications are not federally standardized.

The design team improved the visibility of the driver and effectiveness of bus headlights by placing the rack on the top of the bus. Current bike racks place bikes directly in front of the headlights, which can block some of the light emitted, and the handlebars and seats can be in the way of the front windows, which can block the vision of the driver. The suggested design will eliminate these issues.

As the new system is more complicated to operate than the current styles, it is more likely that riders could need more help with proper operation. The design team should design our system to be intuitive and simple enough for all riders to use on their own and should not require any assistance from the driver. This can ensure that there will be no delays at the stops and the bus can stay on schedule. When a rider lowers the rack and attaches or removes bikes, the rack will be in clear view of the driver. Due to this, they will still be able to ensure proper attachment of the bikes before raising the rack to the roof.

The design team must also consider the implications of adding more space for commuters to store their bicycles on buses. If the design team makes it easier to commute using bicycles and buses, commuters may be more willing to use bikes, which may necessitate the construction of additional bike lanes or designation of sections of existing road for bike lanes. New legislation covering bicycle commuting may also be necessary to ensure the safety of these new commuters. Even though our design accounts for minimal capital and operational costs, the design team should consider these additional costs for bike lane construction or legislation.

Further concerns with the current style of bus bike racks include how the rack affects the bus and its operation since they are add-on units. Manufacturers design racks to be as small and light as possible to minimize their effect on the bus. Therefore, the racks may not be as robust as necessary to last a long time and damaged or worn racks can cause damage to the bus or attached bicycles. Additionally, bus designers did not intend on buses having bike racks mounted on them and therefore, racks can often be in the way of proper maintenance or cleaning of the bus.

Chapter 4. Synthesis and Analysis

4.1. Analysis of Mechanism

The design team began with a mechatronic analysis to analyze the design parameters of the mechanism. The design team performed this analysis using bond graphs and the resultant state equations. The design team later determined that an analysis that utilizes the virtual work method would be easier to analyze our system. This method would also be easier to understand by someone outside of the project. For reference, the mechatronic analysis of a simplified version of the system is in Appendix 6.

The design team analyzed our mechanism using the virtual work method to determine materials and the power the motor must supply. The design team split the mechanism into two different four-bar linkages, a special type Grashof linkage and driver-dyad linkage to determine the power needed. The in-depth calculations and Mathcad code are in Appendix 6.

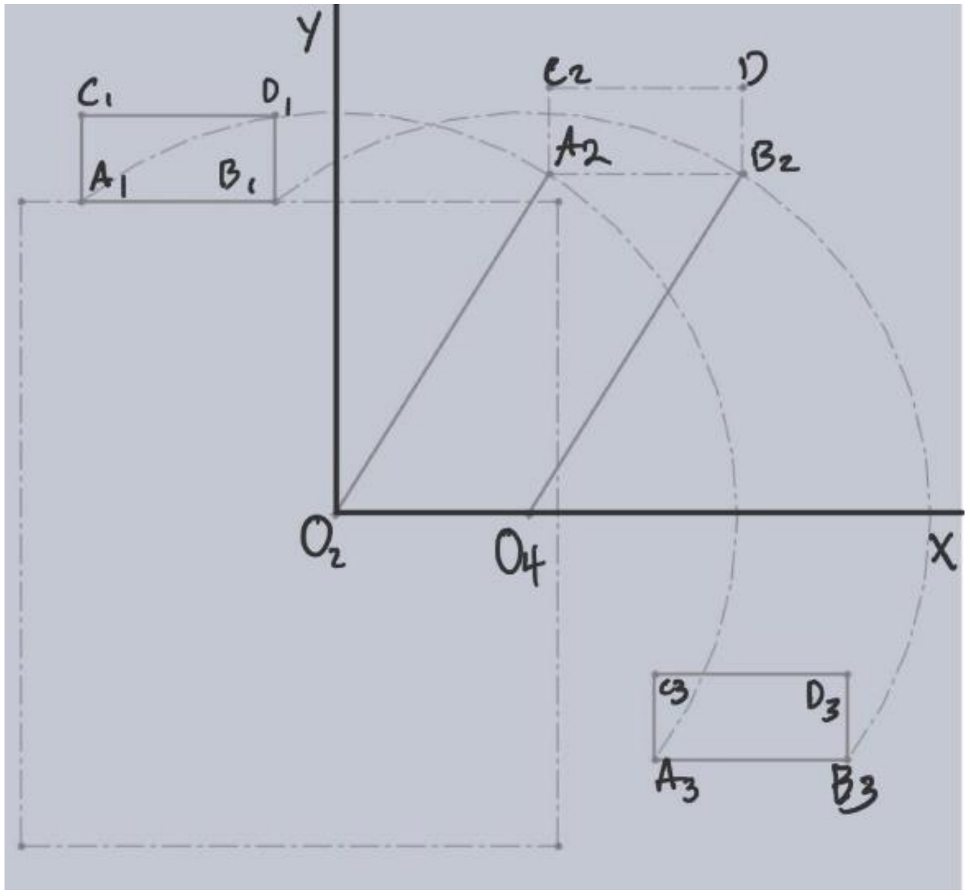

Figure 2: Sketch of Initial Design

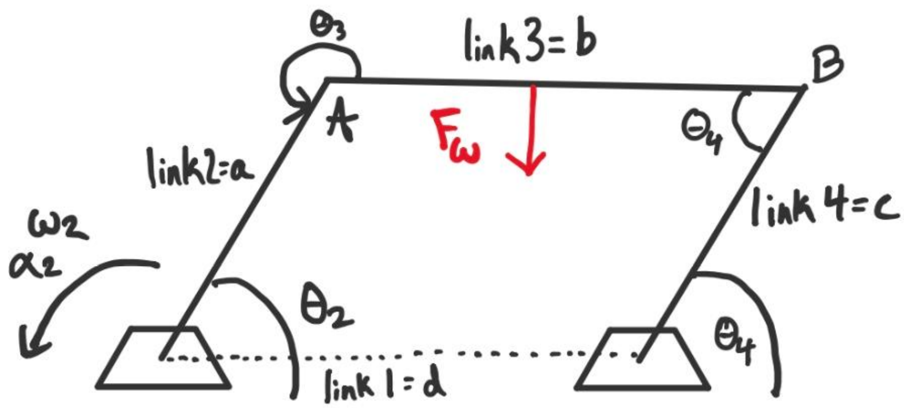

Figure 3: Diagram of a Single Side

The first step for this calculation was to conduct a position and velocity analysis. For our assumptions in this, the design team decided that the input link (Link 2) was moving with a constant angular velocity and had no angular acceleration. Using the angular velocity of link two and the angle of θ_2, the design team were able to conduct a position analysis and find the values for θ_3 and θ_4. The design team were able to determine the angular velocity and acceleration of the links by analyzing their positions. Once the design team solved for the position, velocity, and acceleration the design team used the virtual work method to determine the torque necessary to power our lifter. The design team calculated the torque required using the following equation:

$$T12(\theta 2) := \frac{1}{\omega_2}\cdot\left[\begin{array}{l} m2\cdot(aG2x(\theta 2)\cdot vG2x(\theta 2) + aG2y(\theta 2)\cdot vG2y(\theta 2)) + m3\cdot\begin{pmatrix} aG3x(\theta 2)\cdot vG3x(\theta 2)\ \ldots \\ + aG3y(\theta 2)\cdot vG3y(\theta 2) \end{pmatrix}\ \ldots \\ + m4\cdot(aG4x(\theta 2)\cdot vG4x(\theta 2) + aG4y(\theta 2)\cdot vG4y(\theta 2))\ \ldots \\ + \left(IG2\cdot\alpha 2\cdot\omega_2 + IG3\cdot\alpha 31(\theta 2)\cdot\omega 31(\theta 2) + IG4\cdot\alpha 41(\theta 2)\cdot\omega 41(\theta 2)\right)\ \ldots \\ + [-(FP3x\cdot vP3x(\theta 2) + FP3y\cdot vP3y(\theta 2))] \end{array}\right]$$

In this equation, T_{12} is the torque required as a function of θ_2. The mass of each link is shown as m_2, m_3, and m_4. AG and vG respectively represent the acceleration and velocity of the center of mass for each link. The area moment of inertia for each respective link is displayed as I_G. The angular velocity and acceleration for each link is shown as α and ω, respectively. The external forces present are represented as F. In order to solve for the area moments of inertia, the design team modeled our mechanism in SolidWorks and used the material properties for 80/20 in addition to checking these calculations by hand. The external force present in this mechanism is the same as the weight of the bicycles.

Chapter 5. Design Selection

When initially analyzing the problem, the design team realized that the lifter portion of our mechanism would only be following a single path to take the rack from near-ground-level to the top of the front of the bus. This meant that our design would be the perfect place to implement a four-bar mechanism as it can support the weight of the bike rack effectively while following a single path. The specific type of four-bar mechanism that the team implemented is called a special-type-Grashof linkage. In this linkage, the sum of the lengths of the longest arm and the shortest arm is equal to the sum of the lengths of the two remaining arms. The design team decided on utilizing a special-type-Grashof because the geometry of the arms will keep bikes level while in transit. One of the dangers in using a four-bar mechanism is that the links can become flipped and enter a crossed configuration. This would be dangerous if it were to happen while lifting the bicycles, so the design team added a driver-dyad linkage. The driver-dyad uses one of the pre-existing arms to create a new four-bar linkage. By using this driver-dyad, the design team can control how the mechanism moves and can keep the lifter from entering crossed configuration. In addition to serving as a safety measure, the design team can use the driver-dyad as an input link by attaching a motor to it in order to power our mechanism.

Chapter 6. Detailed Design Description

Our final design consisted of 10 distinct components. The material used for all of our manufactured parts was standard 80/20 T-Slot aluminum with a 1" by 1" face profile. The part drawings were done in SolidWorks and can be found in Appendix 10.2 with our Bill of Materials found below in Figure 6.

ITEM NO.	PART NUMBER	DESCRIPTION	QTY.
1	LONG ARM	1875mm length of 80/20 T-Slot Aluminum	4
2	SHORT ARM	900mm length of 80/20 T-Slot Aluminum	2
3	CONNECTOR	1980mm length of 80/20 T-Slot Aluminum	1
4	REAR CONNECTOR	1853mm length of 80/20 T-Slot Aluminum	1
5	VERTICAL BIKE SUPPORT	152.4mm length of 80/20 T-Slot Aluminum	16
6	HORIZONTAL BIKE SUPPORT	61.4mm length of 80/20 T-Slot Aluminum	8
7	BIKE SUPPORT	1802.2mm length of 80/20 T-Slot Aluminum	12
8	LONG LINK	775mm length of 80/20 T-Slot Aluminum	1
9	SHORT LINK	300mm length of 80/20 T-Slot Aluminum	1
10	1 HP AC MOTOR	1 HP General Purpose Motor,Capacitor-Start,3450 Nameplate RPM,Voltage 115/208-230,Frame 56C	1
Dylan Baker-Flynn	SCALE: 1:1	BILL OF MATERIALS	04/14/2020

Figure 4: Bill of Materials

We decided to utilize 80/20 aluminum as our material of choice because it was readily available on campus and easy to prototype with. The design team was working within a very limited budget and knew the cost of a motor would be significant, so the team reused and recycled as many materials as possible. While our team could have produced a higher quality product using different materials, we decided to remain within our budget and create a prototype that could be easily replicated. For our dimensions, we chose a design that was as compact as possible while still fulfilling all our functional specifications. The length of the Long Arm (Item 1) was determined by the minimum length required to ensure that our design can safely swing in front of the bus without colliding with the top corner of the roof. The length of the Short Arm (Item 2) was based off the minimum length required to store four bicycles side by side. The length of the Connector and Rear Connector (Items 3 and 4, respectively), were based off the width of the bus, and the dimensions required to keep the mechanism from colliding with itself. The dimensions for the Vertical Bike Support, Horizontal Bike Support, and Bike Support were all based off the dimensions required to support the length of the bike and clamp the bike in place just below the axle. Our dimensions for the Long Link and Short Link (Items 8 and 9) were found when the team conducted the mechanism synthesis at the beginning of the project, and the lengths are such that one full rotation of the motor raises and lowers the bike rack.

The main component of the design that the team did not manufacture, was the 1 HP AC motor. This motor was purchased from Grainger and can be seen below in the Exploded Assembly Drawing in Figure 7. When we conducted our analysis of the mechanism using the Virtual Work Method, we learned that we needed a motor with a minimum power output of approximately .5 HP. The team opted to purchase a 1 HP instead of a .5 HP motor because we did not account for the presence of friction and other imperfections in the system during our analysis, and a 1 HP motor was the next economically viable motor available motor available for purchase. Due to the skillsets of our team members, we opted to use a motor that could be plugged into the wall and run at 120 Volts AC rather than figuring out another way to provide power to the motor.

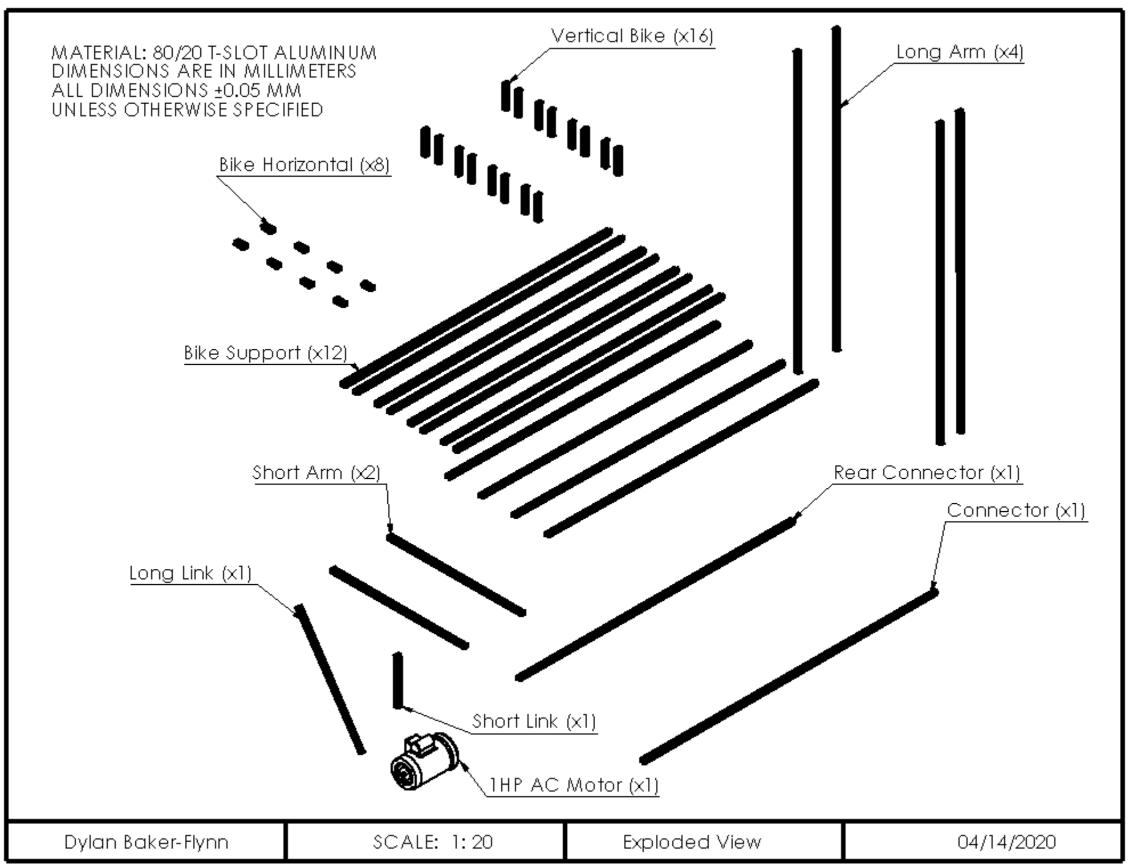

Figure 5: Exploded Assembly Drawing

Chapter 7. Manufacturing

The design team built a half-scale model to test our design and determine the legitimacy of the analysis completed. The design team began with a base constructed of plywood and two-inch by four-inch wooden members (two-by-fours). This base takes the place of a half-scale bus model. The final rack lifter will not include this base section, as the design team will attach the links to the bus directly.

The design team selected plywood and two-by-fours, as they were both cheap and easy to use to build a stable base. The design team used a handsaw and a cordless drill in the Washburn Shops and Foisie Innovation Studio Makerspace. Figure 6 shows the base after construction at the Foisie Innovation Studio Makerspace at WPI. Though it is difficult to see, each vertical two-by-four has a hole drilled near the top to attach the links of the four-bar linkage.

Figure 6: Half-scale Model Base

The design team constructed the links and the frame of the rack that will hold the bicycles from 80/20 T-slot Aluminum extrusions. These extrusions were selected for their ease of use in prototyping and were sourced from a previous on-campus project. The design team cut the extrusions to length using a horizontal band saw and filed the cut ends using hand files.

Figure 7: Links Made of 80/20 Extrusion

Figure 8: Horizontal Band Saw Cutting 80/20

Once the links were cut to length from the 80/20, holes were drilled through to match up with the link lengths of our CAD design and the Mathcad calculations. These were then attached to one another with 90-degree brackets to make up the general frame of the rack. 3/8 inch bolts, washers, and nylon locknuts were used to attach the links to the rack and to the two-by-fours acting as the points of contact on the bus.

7.1. Future Manufacturing

Due to unprecedented limitations of time and resources, the team was unable to complete the manufacturing of the prototype. While the majority of the manufacturing and assembly was accomplished, the remaining tasks can be divided into two categories, necessary to work and optimization. The majority of our progress can be seen below in Figure 11.

Figure 9: Prototype of the Device

In order to finish our prototype, we would need to finish the assembly of the driver dyad and finish the manufacturing of the bicycle mount itself. To finish the driver dyad, we need to drill holes as seen in the part drawings for Short Link and Long Link in Appendix 10.2. The 3/8” holes are used to connect the links together, as well as connect the Long Link to the Long Arm part of the four-bar mechanism. The 5/8” hole attaches directly to the motor and is held in place by the 3/16” key. While the 3/8” holes can be drilled with the standard tooling available in Washburn Shops, we ordered a special 5/8” steel drill bit, which we intended to use to create the slot for the motor. To create the bike mounts, we would have followed the part designs found under Bike Supports in Appendix 10.2. These bike mounts were designed to clamp the wheels of a standard bike just below the axle and were accommodate the average road bike’s tire, which ranges from approximately 28mm to 36mm.

After our initial construction, we developed a list of ways to improve our mechanism. The first and most significant change was to switch the two rear Long Arms to be inside of the wooden supports. In order to accomplish this change, we would have removed 5 inches from the Rear Connector (3 inches for the width of two

2-by-4s, and 2 inches for the width of two 80/20 bars). The two main reasons for this swap were to help reduce friction from the Long Arms rubbing against the wood, as well as to avoid collision when the Long Arms were at certain angles. In addition to changing the placement of the rear Long Arms, we proposed to use nylon spacers to help reduce the friction present in the four-bar mechanism. When the Long Arms connect to the Connector and Rear Connector, there is a 3/8" hole drilled into the Long Arms, which allows a bolt to slide through and be threaded in to the Connector and Rear Connector. To alleviate the friction present from the 80/20 rubbing on the bolts, we planned to use a tube of nylon or another smooth material with a low coefficient of friction with an outer diameter of 3/8" and an inner diameter of 1/4".

Chapter 8. Testing

As the effects of the pandemic surround the coronavirus limited us, we were unable to complete the manufacturing and resultant testing of our device. With the device at the status it was left before we had no further access to machine tools or additional materials for its completion, we completed some analysis on whether we believe that the rack lifter would be able to accomplish the intended functions. In order to best visualize how our mechanism would have worked, we simulated the motion of the bike rack using SolidWorks and submitted this animation to the Virtual Research Showcase as part of our presentation. The animation of our model showed the potential of the model we were in the process of building. Since a full rotation of the motor will lower and raise the bike rack, we only need to use a half rotation to move the rack into either position. Running at a lower level of power, the optimal rotational speed for the motor is 10 rotations per minute as this is where the bike rack moves slow enough where it is not dangerous to its operator, and quick enough that it does slow down the bus. If the machine shops had not been shut down, we are confident the mechanism would have functioned as designed.

Chapter 9. Conclusions and Recommendations

Unfortunately, due the circumstances related to the COVID-19 pandemic, we were unable to finish our project. While we were able to construct the majority of our model, the closure of the machine shops on campus and lack of access to power tools left our team with very limited options. We are confident that if we had access to the tools required, our project would have fulfilled the functional requirements we set.

When working with the model we had constructed, we realized that the primary weakness was an excess amount of friction present in the system. Before we learned that the machine shops were closed starting in D-term, we developed a list of improvements we wanted to implement that would help reduce the friction present. These improvements are covered in Section 7.1 Future Manufacturing and were mostly based on small redesigns that would not require a significant overhaul to our project. The two major changes to the design were staggering the placement of the Long Arms, and the creation of low-friction bushings. The reason for staggering the placement of the Long Arms was so that we could avoid collisions between both sets of Long Arms, and so it would reduce the friction present when the 80/20 rubbed against the wooden support beams used for our prototype's base. The low-friction bushings were meant to be used in the rotational joints of the four-bar mechanism. These could be manufactured out of a low-friction material like nylon, and would have bolts threaded through them to hold the mechanism together.

If we were given the ability the restart this project, we would have started the manufacturing and testing of our mechanism earlier. The primary issue we ran into while working on this project was losing access to the resources available on campus for manufacturing. When starting this project we created a schedule for all four terms with our research taking place in A-term, our analysis and design taking place in B-term, the majority of our manufacturing taking place in C-term, and our testing and iteration taking place in D-term. If we had prior knowledge that we would lose access to the manufacturing resources on campus, we would have revised our schedule so the research, analysis, and design took place side by side in A-term, leaving B-term and C-term open for our manufacturing and testing.

9.1. Recommendations for Further Design

The design that the team was able to come up with in the past 9 months forms a basis for what could become a useful device in the future. As movements towards sustainability continue, it is likely that bike-to-bus commuting and similar forms of transportation will increase even more and the need for technology such as this will become even more valuable. In addition, the later implementation of improved bus bike racks could be designed in conjunction with newer, more energy-efficient, designs for buses and the “ideal solution” suggested in Chapter 3 could become reality.

There are a few recommendations for further work on this project as the team was unable to complete manufacturing and perform any sort of extensive testing of the prototype half-scale model. First, the use of bearings on the joints of the linkage could reduce the high levels of friction that we experienced when testing the motion. This reduction in friction present would better represent the motion of the final device, and a more efficient model could potentially lower the power requirements for the motor. Second, the use of higher quality materials for a next prototype could also better represent the real-life device and allow the design team to have a better idea of what the actual operation of the device would be when in use. Higher quality materials also would have allowed us to manufacture more customizable parts, because although the 80/20 aluminum we used is wonderful for rapid prototyping it is limited in its manufacturing capabilities. A full-scale model is another recommendation that could allow for testing using materials that could be used on the final device. A full-scale model could also allow the design team to perform stress testing using full-size bicycles on the rack.

Chapter 10. Appendices

10.1. Glossary

Standover height – height of the top horizontal bar of a bicycle

Two-by-four – wooden member with an approximate cross section of two inches by four inches

80/20 – aluminum T-slot structural framing produced by 80/20 Inc. for modular construction.

10.2. Part Drawings

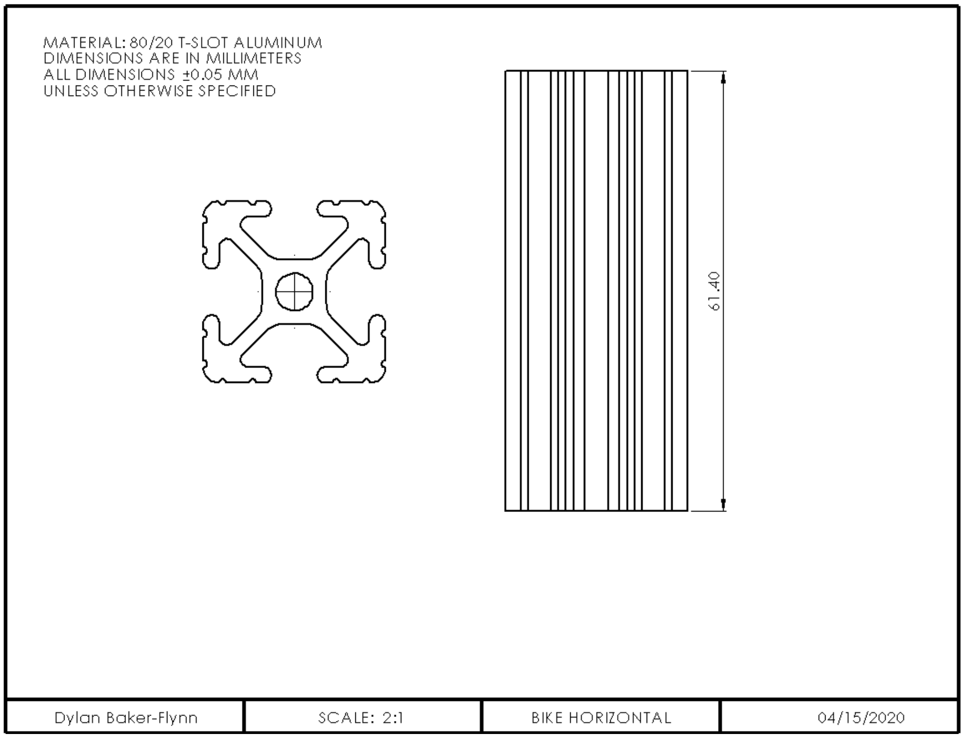

Figure 10: Bike Horizontal Part Drawing

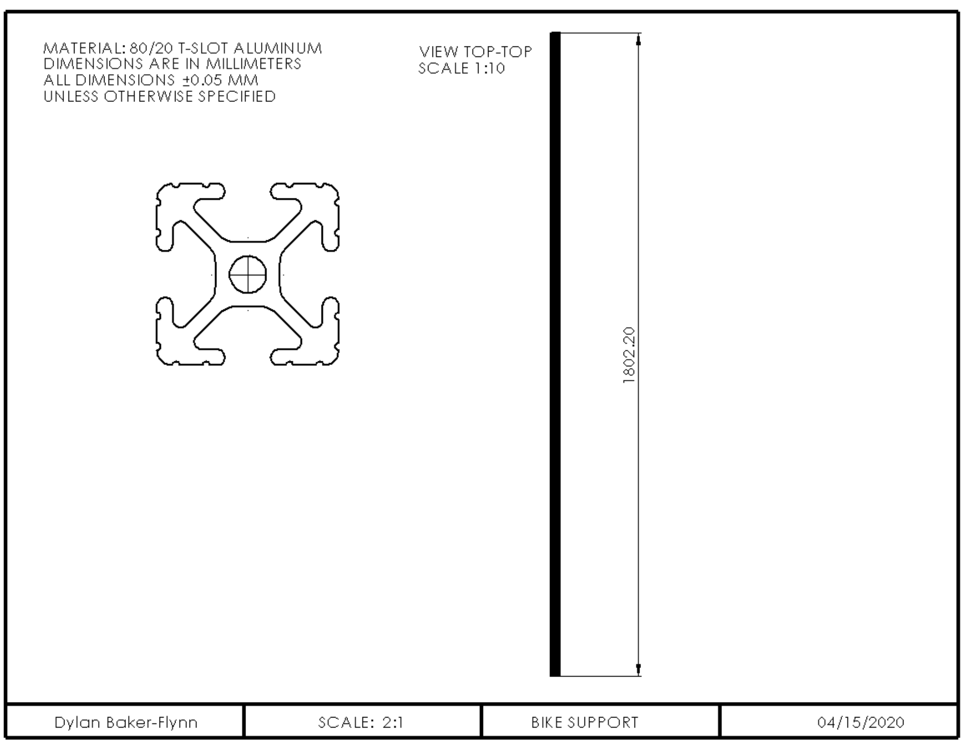

Figure 11: Bike Support Part Drawing

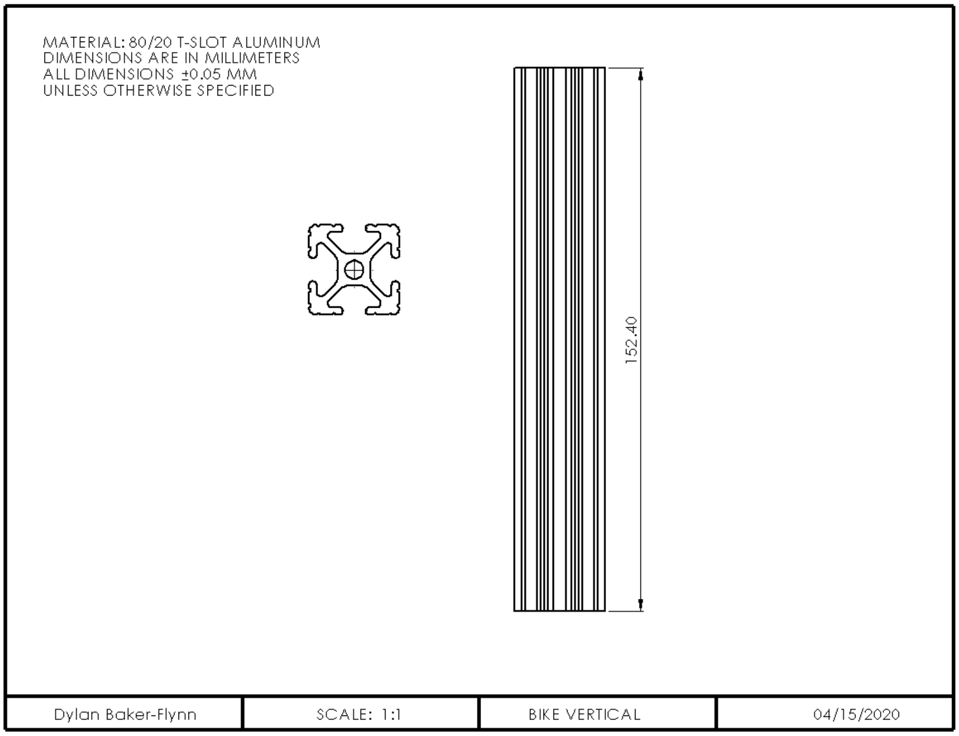

Figure 12: Bike Vertical Part Drawing

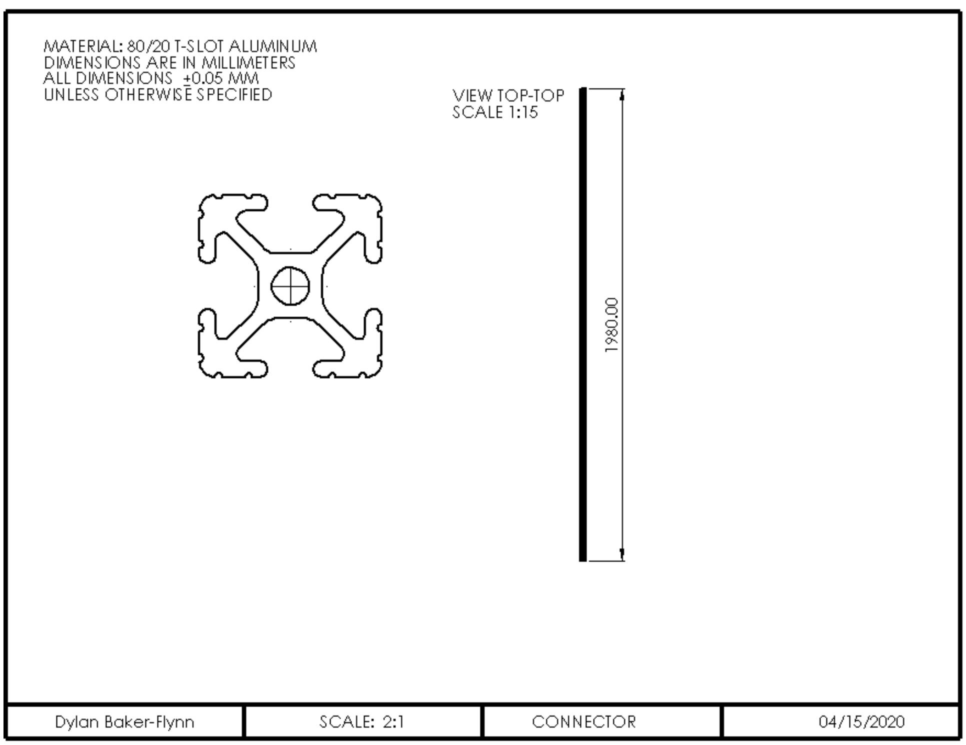

Figure 13: Connector Part Drawing

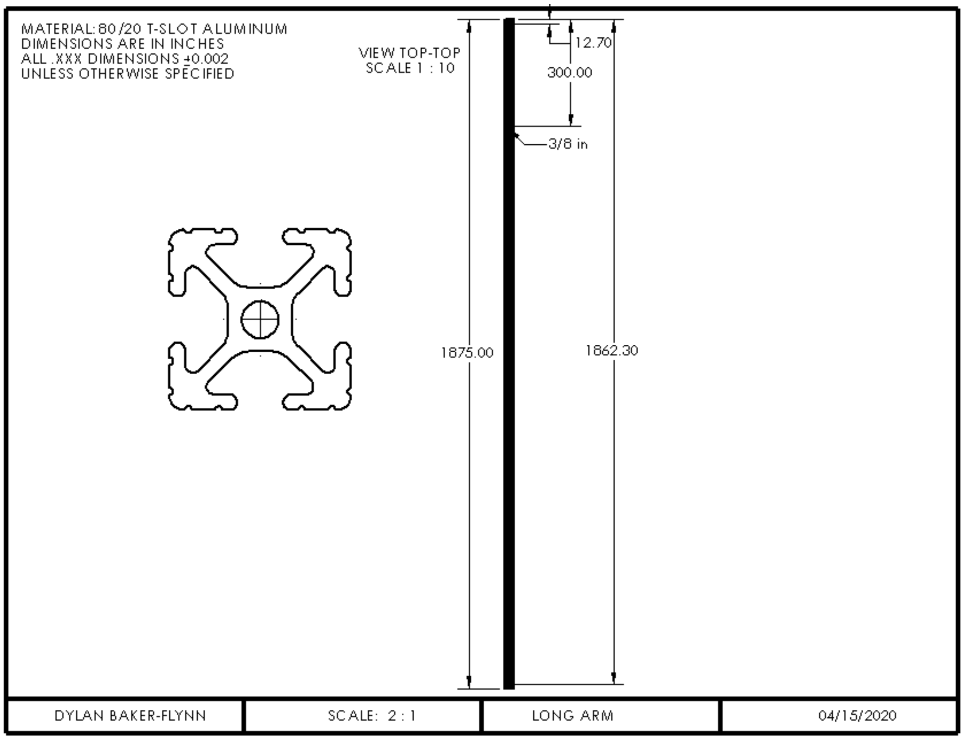

Figure 14: Long Arm Part Drawing

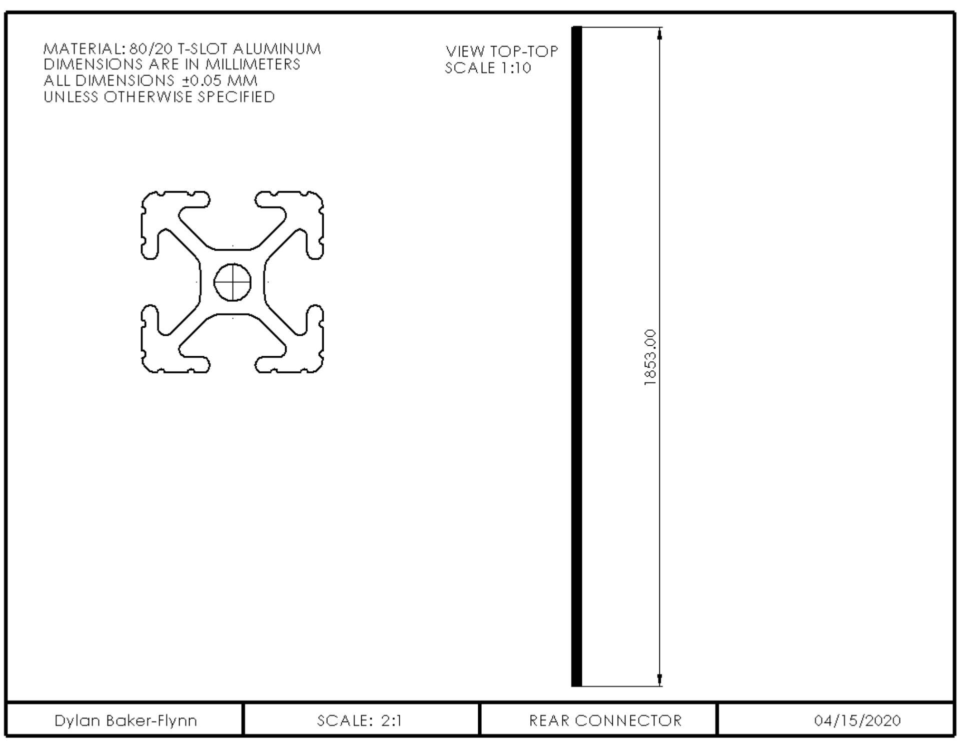

Figure 15: Rear Connector Part Drawing

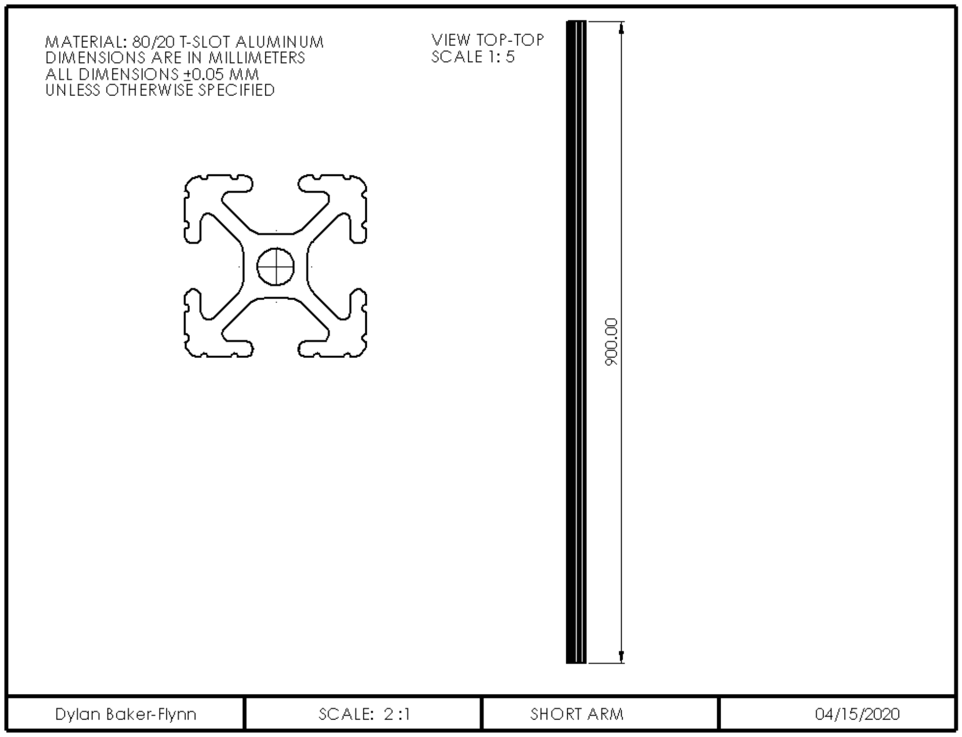

Figure 16: Short Arm Part Drawing

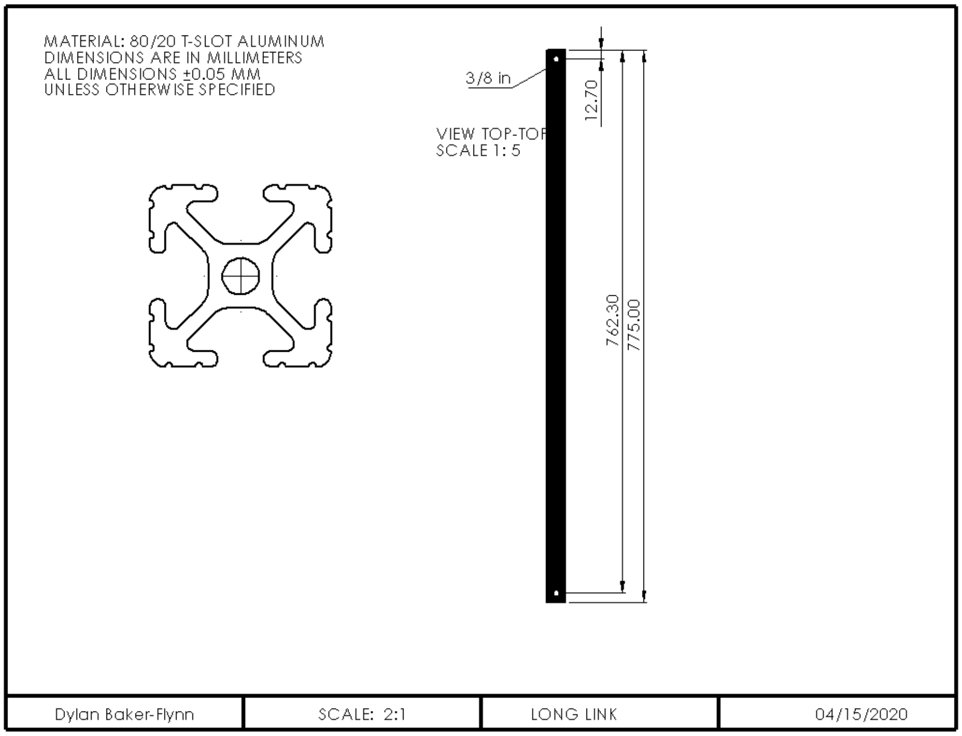

Figure 17: Long Link Part Drawing

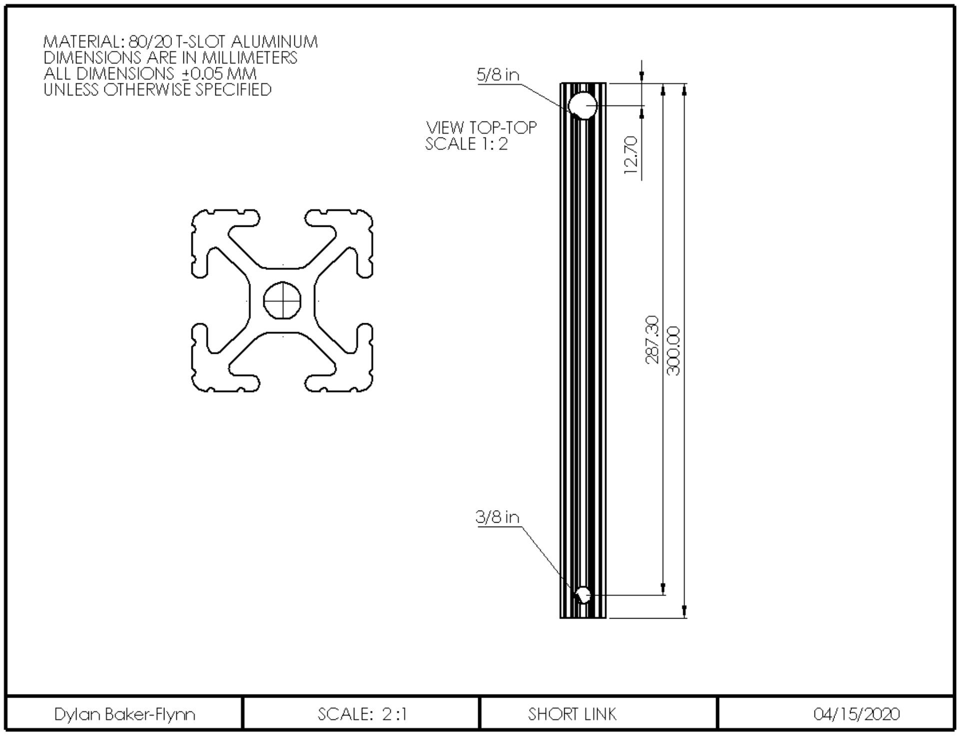

Figure 18: Short Link Part Drawing

10.3. Assembly Drawings

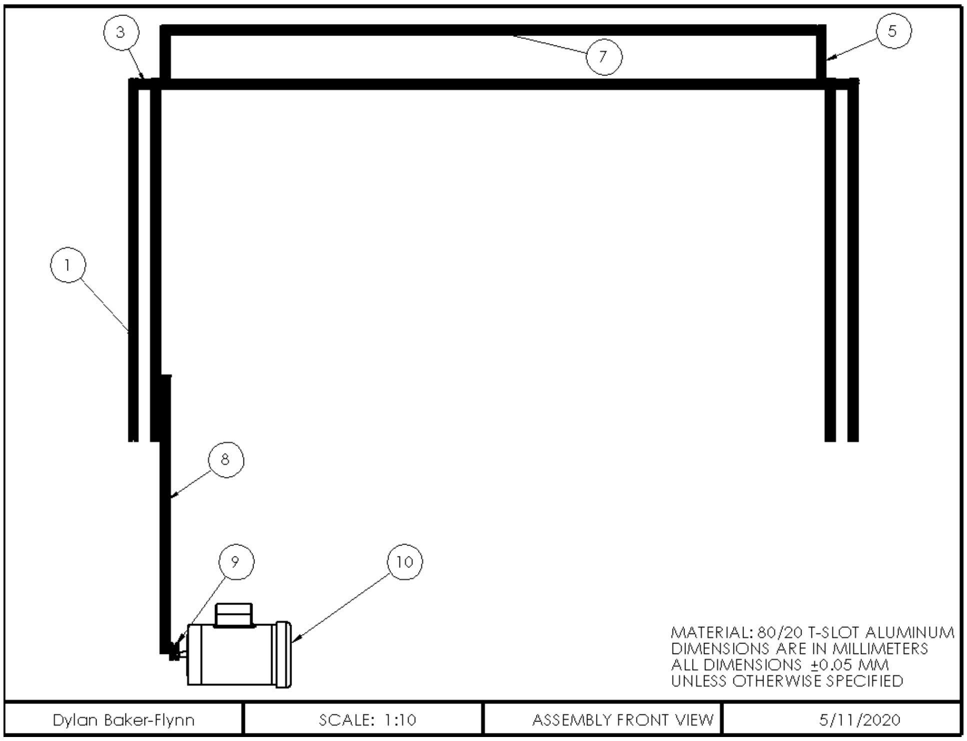

Figure 19: Assembly Front View

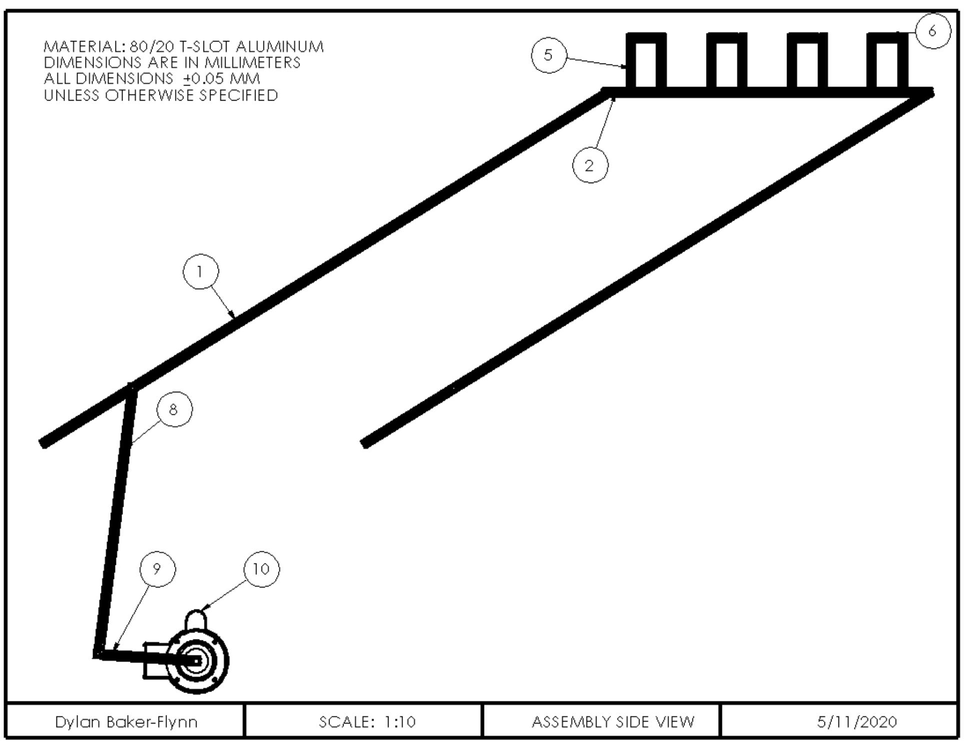

Figure 20: Assembly Side View

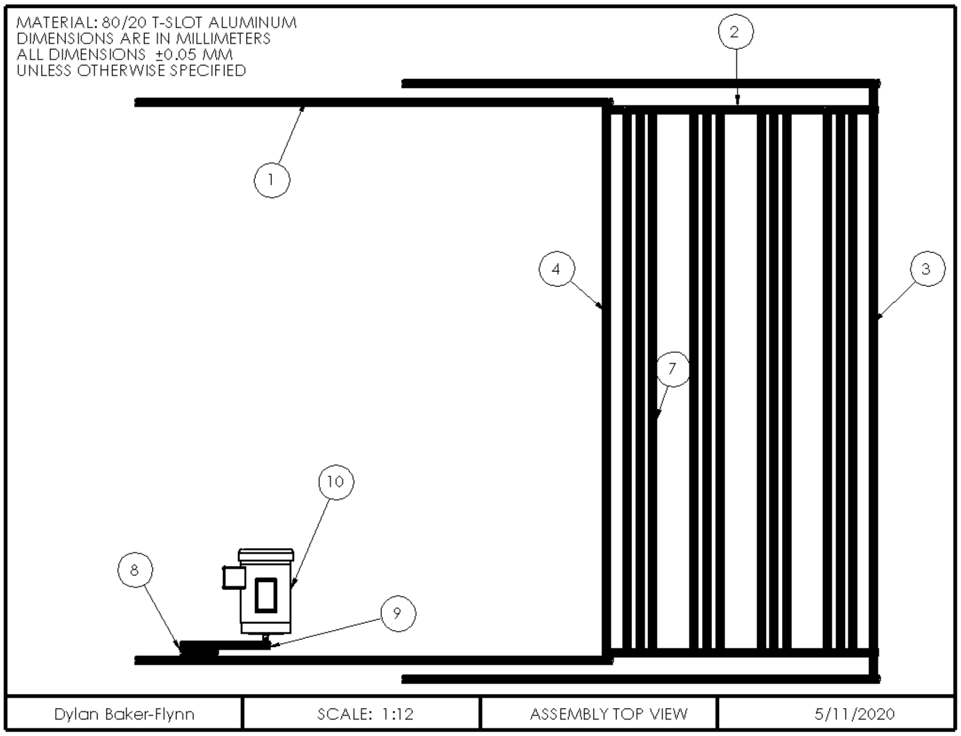

Figure 21: Assembly Top View

10.4. Authorship

Section #	Section Title	Primary Author(s)	Primary Editor(s)
	Abstract	Cole Flegel	Cole Flegel
	Acknowledgements	Cole Flegel	Cole Flegel
1.	Introduction	Cole Flegel	Cole Flegel, Dylan Baker-Flynn
1.1.	Expected Outcome	Cole Flegel	Cole Flegel
1.2.	Client Statement	Cole Flegel	Cole Flegel, Dylan Baker-Flynn
2.	Background	Cole Flegel	Cole Flegel
2.1.	Current Practices	Cole Flegel	Cole Flegel, Dylan Baker-Flynn
2.2.	Issues with Current Practices	Cole Flegel	Cole Flegel
2.3.	Legal Parameters	Cole Flegel	Cole Flegel, Dylan Baker-Flynn
2.4.	Bicycle Parameters	Cole Flegel	Cole Flegel, Dylan Baker-Flynn
2.5.	Human Parameters	Cole Flegel	Cole Flegel, Dylan Baker-Flynn
2.6.	Functional Specifications	Cole Flegel	Cole Flegel, Dylan Baker-Flynn
3.	Design Concepts	Cole Flegel	Cole Flegel, Dylan Baker-Flynn
3.1.	Design	Cole Flegel	Cole Flegel, Dylan Baker-Flynn
3.2.	Solving Issues	Cole Flegel	Cole Flegel, Dylan Baker-Flynn
4.	Synthesis and Analysis	Dylan Baker-Flynn	Cole Flegel
5.	Design Selection	Dylan Baker-Flynn	Cole Flegel
6.	Detailed Design Description	Dylan Baker-Flynn	Cole Flegel
7.	Manufacturing	Cole Flegel	Cole Flegel
7.1.	Future Manufacturing	Dylan Baker-Flynn	Cole Flegel
8.	Testing	Dylan Baker-Flynn	Cole Flegel
9.	Conclusions and Recommendations	Dylan Baker-Flynn	Cole Flegel
10.1.	Glossary	Cole Flegel	Dylan Baker-Flynn
10.2.	Part Drawings	Dylan Baker-Flynn	Cole Flegel

10.3.	Bibliography	Cole Flegel	Dylan Baker-Flynn
10.4.	Assembly Drawing	Dylan Baker-Flynn	Dylan Baker-Flynn
10.6.	Mechatronic Analysis	Cole Flegel, Maricella Ramirez, Jianqing Zhu	Cole Flegel
10.7	Calculations	Dylan Baker-Flynn	Dylan Baker-Flynn

10.5. Mechatronic Analysis

To determine the necessary parameters of the four-bar linkage and the gearbox necessary to drive it, Cole Flegel, Maricella Ramirez, and Jianqing Zhu, all of WPI, performed a mechatronic analysis. As it turned out to be much more difficult for an advanced system such as the drag-link four-bar linkage than anticipated, the design team disregarded this analysis for a Mechatronic analysis as a method of solving for the significant values of a system that has both mechanical and electronic components. The basic steps of the analysis are:

1. Draw a system diagram of the complete system.
2. Determine the locations of velocities of mechanical sections and voltages of electronic sections of the system.
3. Generate bond graph using different components of the system.
4. Apply causality to bonds.
5. Designate states in integral causality.
6. Solve the state equations for each state in integral causality.
7. Combine the state equations to form differential equations that can help us to solve for values necessary for the design of our lifter.

10.5.1. Background

Bond graphs consist of a variety of nodes connected with directional bonds. In the center of the graph, ones and zeroes designate nodes. The ones represent the velocities between mechanical components and the locations of electronic components. The zeroes represent the locations of mechanical components and the voltages between electronic components. On the outside of the graph, different components are represented by capital letters. An R represents a resistive element, either an electronic resistor or the damping of a mechanical component. A C represents a storage element, such as an electronic capacitor or mechanical spring. An I represents an electronic inductor or the mass moment of inertia of the mechanical rotation of a component. An M represents the mass of a component

The simplified system that the design team used for this analysis consists of 3 main subsystems, a drag-link four-bar linkage (Fig. 2), an electric motor, and a gearbox consisting of 5 stages (Fig. 1). The gearbox has an overall gear reduction of 1800:1 to decrease the output velocity of the electric motor and increase the torque output at the coupler link of the linkage.

System diagrams of the gearbox and four-bar linkage (Figures 4-5) were drafted to illustrate the overall relationship between the input torques and output forces. The diagrams are based strictly off the gearbox necessary to convert the torque of an 1800 rpm input motor to the output torque needed for proper motion of the linkage.

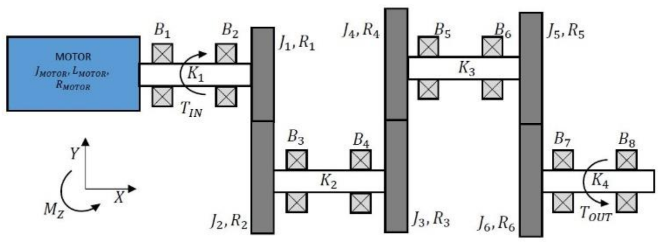

Figure 22: System Diagram of Gearbox with Motor

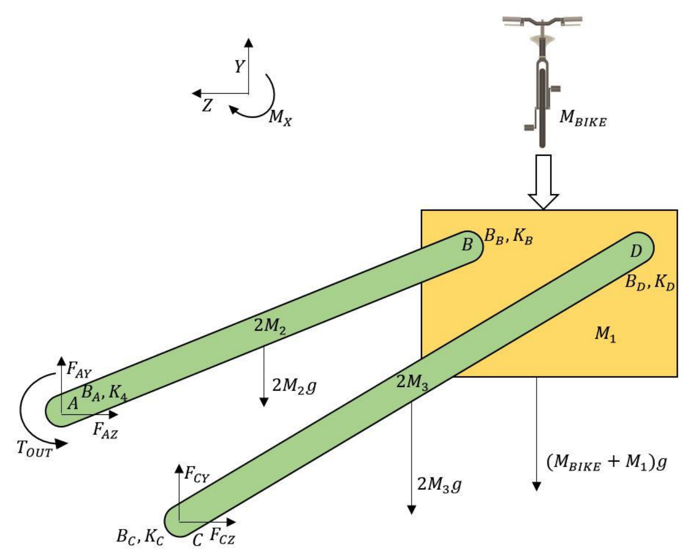

Figure 23: System Diagram of Four-bar Linkage

10.5.2. Assumptions

As there are many parameters that can change, the design team made some assumptions to simplify our analysis of the mechatronic system. Since the mechanism is symmetrical about the middle, the design team are going to analyze one side of it. If desired later on, the design team can easily modify the analysis along the symmetry. As our mechanism is large and will often be at a great distance above the ground, the design team must assume gravity effects on all major components of the system. The friction of all moving parts is considered in our modeling. The shafts in the gearbox will be considered have certain spring coefficient. However, the linkages will be considered as rigid parts.

The design team are assuming the system is powered by the city bus with electricity and will be using an electric motor to operate. the design team will also consider the motor, gearbox, and linkages design parameter in further completion of the project. Finally, as the weight on the coupler Link *BD* can change due to different amounts of bikes held on the rack, the design team will assume a standard weight of X bikes and the weight of Link *BD* as the total mass of Link *BD*.

In order to calculate spring, damping and inertia an estimate of the mechanical design of the system. The average height of a bus is 10 ft., and taking into account reasonable height of the linkage's installment, the links for this system would be around 7 ft. in length, width of 5 inches and thickness of 2 inches. The bearings used are likely to be 2 inch bore bearings. Data of this type of bearing was taken from the Damping Coefficient Reports in the course resources [10]. Finally, the shafts used at the joints were estimated to be about 2.165 inches or 55 mm in diameter and have the same thickness of the linkages, 2 inches. The material of linkages and shafts was decided to be industrial steel, which has a modulus shear of 79.3 GPa **[7].**

10.5.3. Free-Body Diagrams

Figures 5 and 6 provide representative free-body diagrams of a gear and shaft with attached gear, respectively. These diagrams apply to each gear and shaft in the gearbox.

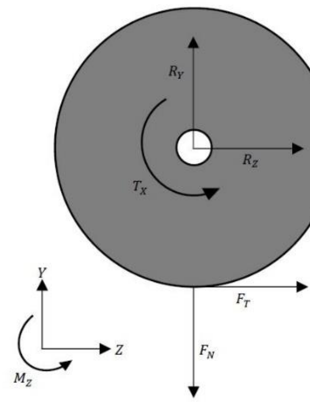

Figure 24: Free Body Diagram of Representative Gear

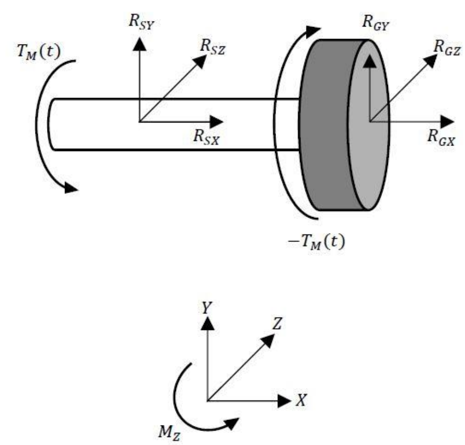

Figure 25: Free Body Diagram of Representative Shaft with Attached Gear

Figures 7-9 are free body diagrams of each link in the four-bar linkage, apart from the ground link of the bus body. Links *AB* and *CD* connect the bike rack to the bus and act as the output and input cranks of the system, respectively. Link *BD* is the rack, which carries the bicycles and is a floating link carrier of the linkage.

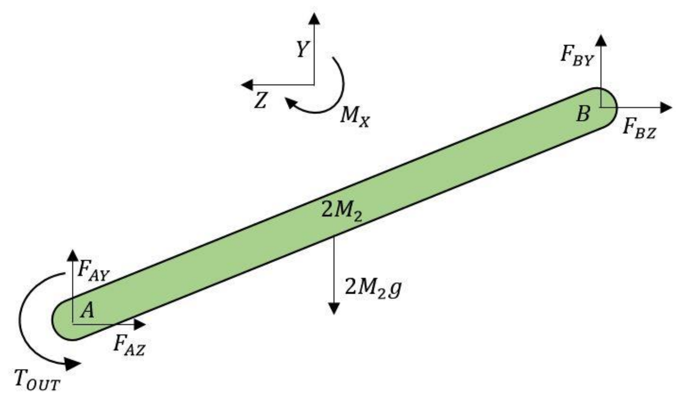

Figure 26: Free Body Diagram of Link AB

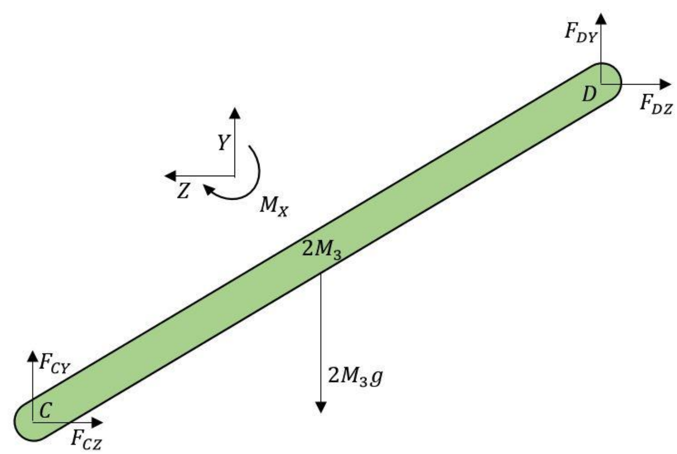

Figure 27: Free Body Diagram of Link CD

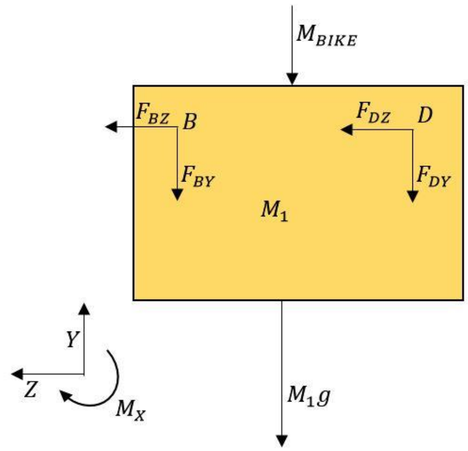

Figure 28: Free Body Diagram of Link BD *(Bike Rack)*

10.5.4. Dynamic Response

The design team are focusing our dynamic analysis on the four-bar linkage system as shown below. The joints *A* and *C* are grounded. Link *BD* will stay horizontal at all time of operation. The design team are assuming at joint *C*, there is a constant angular velocity input. The design team are expecting to derive equations 1 and 2 to find the position of the COM (center of mass) of Link *AB* at certain time point. Then the design team can derive the input torque required by calculating the angular momentum of the Link *AB*.

$$x' = f(\theta') \quad (1)$$

$$h(t) = f(T(t)) \quad (2)$$

10.5.5. Bond Graph

Based on the full four-bar linkage system pictured in Figure 11, a block diagram of the linkage was drafted as shown in Figure 13. The DC motor that ran the system was modeled as a permanent magnet DC motor, shown in Figure 12.

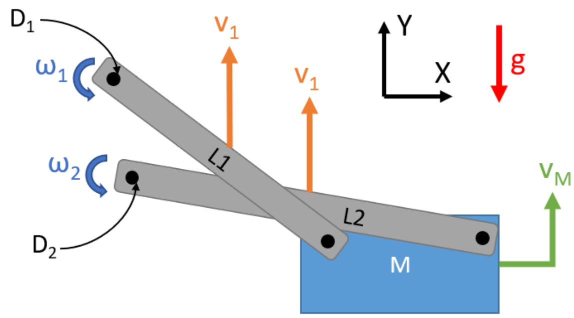

Figure 29: Block Diagram of Four bar Linkage

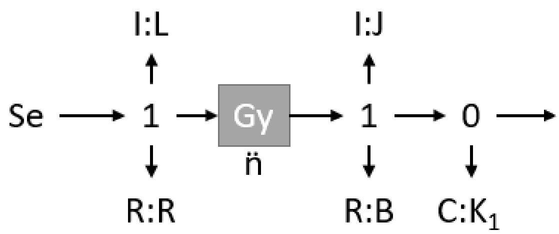

Figure 30: Block Diagram of Four bar Linkage

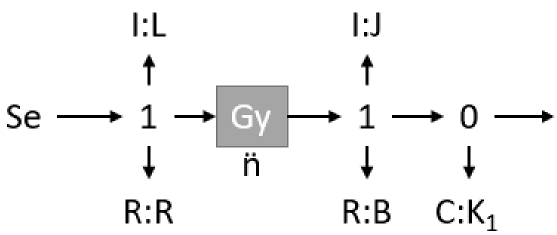

: Bond Graph of Permanent Magnet DC Motor

The initial draft of the bond graph, shown in Figure 13, considered the links with plane motion, and not the rack, which is the couple link.

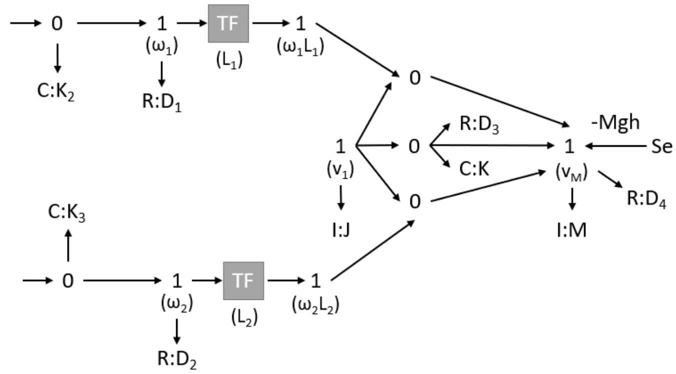

Figure 31: Initial Bond Graph of Four bar Linkage

The initial draft is flawed in that it disregards the plane motion happening on the rack and fails to represent the relation between links and velocities. An example of a correct bond graph of a four bar linkage is shown in Figure 14 **[4].**

The bond graph for the linkage was created using the example in Figure 13. In this model of a four bar linkage, the coupler link is considered an *I* element 3 times, once as *M* for the x direction (V_y), *M* for the y direction (V_y) and as *J* for the rotational motion (θ_3).

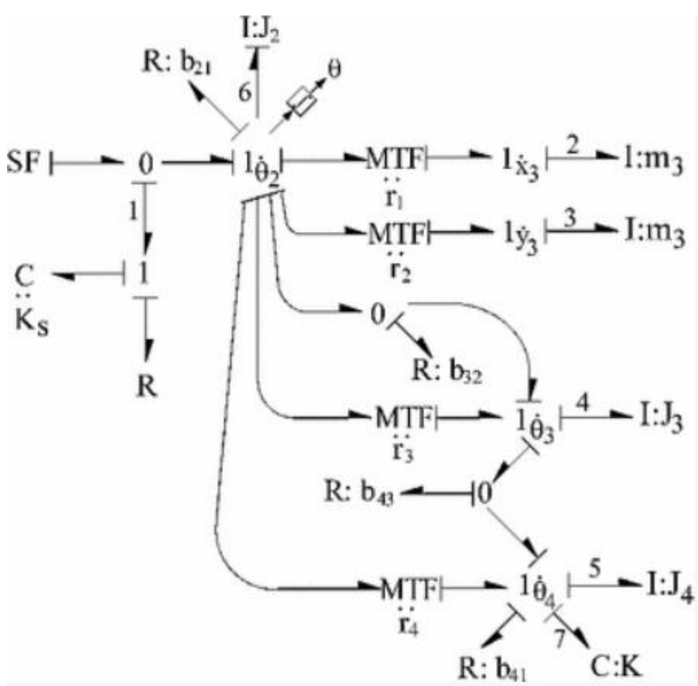

Figure 32: Example of Correct Four Bar Linkage Bond Graph

There are nine states in the system bond graph, represented as elements highlighted in green in Figure 12. In order to make several I elements integral, soft padding was used in the bond graph. The soft padding elements are considered to be any compliance and damping at the joints of the system as well as within the rack itself.

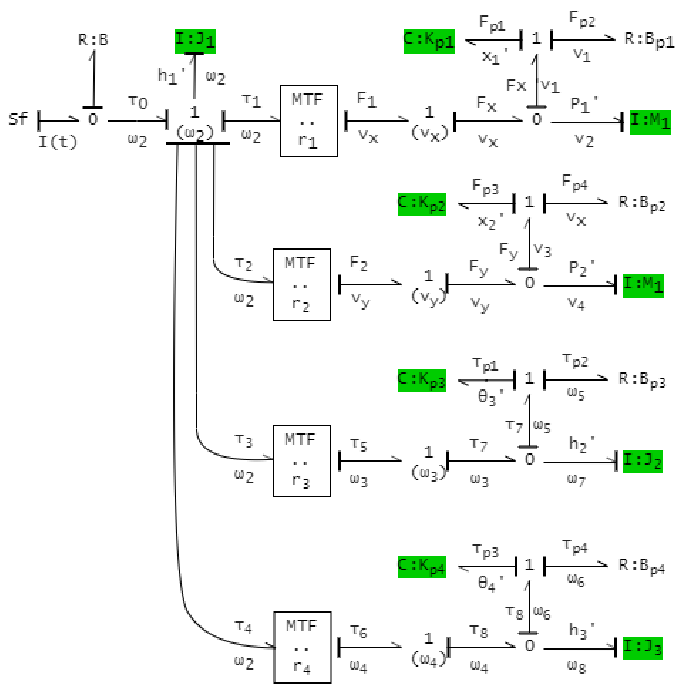

Figure 33: Causal Bond Graph of the System

10.5.6. State Equations

The state equations for this system are $h_1(t), h_2(t), h_3(t), p_1(t), p_2(t), x_1(t), x_2(t), \theta_3(t)$, and $\theta_4(t)$. Thes equations are written out below. The terms τ_1, τ_2, τ_3, and τ_4 are used frequently therefore will be written out in their entirety below but not when used in the state equations.

$$\tau_1 = -r_1 \cdot (k_{p1} \cdot x_1 + \left(B_{p1} \cdot \left(\left(r_1 \cdot \frac{h_1}{J_1}\right) - \frac{p_1}{M_1}\right)\right)) \tag{3}$$

$$\tau_2 = -r_2 \cdot (k_{p2} \cdot x_2 + \left(B_{p2} \cdot \left(\left(r_2 \cdot \frac{h_1}{J_1}\right) - \frac{p_2}{M_1}\right)\right)) \tag{4}$$

$$\tau_3 = -r_3 \cdot (k_{p3} \cdot \theta_3 + \left(B_{p3} \cdot \left(\left(r_3 \cdot \frac{h_1}{J_1}\right) - \frac{h_2}{J_2}\right)\right)) \quad (5)$$

$$\tau_4 = -r_4 \cdot (k_{p4} \cdot \theta_4 + \left(B_{p4} \cdot \left(\left(r_4 \cdot \frac{h_1}{J_1}\right) - \frac{h_3}{J_3}\right)\right)) \quad (6)$$

$$h_1' = \tau_0 - \tau_1 - \tau_2 - \tau_3 - \tau_4 \quad (7)$$

$$p_1' = \frac{\tau_1}{r_1} \quad (8)$$

$$p_2' = \frac{\tau_2}{r_2} \quad (9)$$

$$x_1' = \left(r_1 \cdot \frac{h_1}{J_1}\right) - \frac{p_1}{M_1} \quad (10)$$

$$x_2' = \left(r_2 \cdot \frac{h_1}{J_1}\right) - \frac{p_2}{M_1} \quad (11)$$

$$h_2' = \frac{\tau_3}{r_3} \quad (12)$$

$$h_3' = \frac{\tau_4}{r_4} \quad (13)$$

$$\theta_3' = \frac{r_3 \cdot h_1}{J_1} - \frac{h_2}{J_2} \quad (14)$$

$$\theta_4' = \frac{r_4 \cdot h_1}{J_1} - \frac{h_3}{J_3} \quad (15)$$

10.5.7. Calculation of Values

We began using transformer moduli to calculate critical values for the system. L_5 is the length of Link *BD,* which is not constant. L_1 is the length of the ground link *AD.* The angle between Link *AB* and the ground link *AD* is θ_2. The angle between L_5 and the ground link *AD* is α. Using this geometry the design team can solve these equations to solve for the modulus r_4. This technique can be applied to the geometry of the entire linkage to solve for all transformer modulus.

$$L_2 \cdot sin(\theta_2) = L_5 \cdot sin(\alpha) \quad (16)$$

$$L_2 \cdot \cos(\theta_2) - L_5 \cdot \cos(\alpha) = L_1 \qquad (17)$$

If the two equations above are solved to obtain L_5 and α as functions of θ_2 the design team can determine the angle between *BCD* and Link *AD,* which is ρ. With ρ, the design team can take the derivative on both sides of the following equation to obtain the transformer modulus r_4 **[4].**

$$\theta_4 = \alpha - \rho \qquad (18)$$

$$M = p \cdot L \cdot b \cdot h \qquad (19)$$

$$M_{link} = 0.284\, {}^{lb}/_{in^2} \cdot 84in \cdot 5in \cdot 2in = 238.56lb \qquad (20)$$

$$M_{rack} = 0.284\, {}^{lb}/_{in^2} \cdot 60in \cdot 5in \cdot 2in = 5112lb \qquad (21)$$

$$J = \frac{M \cdot (L^2 + h^2)}{12} \qquad (22)$$

$$J_1, J_3 = \frac{M_{link} \cdot (84in^2 + 2in^2)}{12} = 140352.8lb \cdot in^2 \qquad (23)$$

$$J_2 = \frac{M_{rack} \cdot (60in^2 + 2in^2)}{12} = 1535304lb \cdot in^2 \qquad (24)$$

$$K_{shaft} = \frac{\pi \cdot d^4 \cdot G}{32 \cdot L} \qquad (25)$$

$$K_{shaft} = \frac{\pi (55mm)^4 (79.3 \cdot 10^{-3})}{32(50.8mm)} = 1402N \cdot mm \qquad (26)$$

The damping coefficient for the bearings was estimated based on course resources. The graphs in Figure 15 show the relationship between the RPM and the temperature, damping, and stiffness of a 2-inch-bore tapered bearing, which just happened to be about the size required for the linkages. The compliance was attributed to shafts instead of the bearings, therefore only the damping was considered.

Because the RPM at the joints and output would be different, the RPM at the input joint was the benchmark. According to Figure 16, an input RPM of approximately 1,800 RPM would translate to about a damping coefficient of 3,000 Ns/m at that joint [10].

From the state equations, the design team solved a series of differential equations. Using MATLAB, the design team were able to determine the values associated with the bond graph… The full MATLAB script is found in Section 9 of Appendix 5.

10.5.8. Discussion

The many variable factors of the system made this system rather challenging to create the bond graph and state equations. The design team had previously assumed a much simpler analysis using many assumptions, however, many of the assumptions simplified the system too much and made the analysis inaccurate. Using a design that was not complete and did not have exact specifications and details of the components proved very difficult, as the design team had to determine our own specifications and details in addition to the analysis itself. That said after looking at the principles found in the text for representing a four bar linkage, a more accurate analysis could be conducted. The state equations obtained required the use of soft-padding, which unexpectedly transformed the representation to achieve nuance that could be seen as more realistic. The last step of this project is solving the state equations after applying constants and initial conditions and finding how velocity of the rack vary over time. With MATLAB programming, this can be done in a relatively more efficient way. This analysis of the bus bike rack lifter system will prove very valuable to the MQP group that is designing the mechanism and it can be applied and modified as necessary to solve for factors of the design, such as the necessary input torque to the linkage.

10.5.9. MATLAB Script

```
% Initial conditions and constants

T_0=17.52; % input torque from gearbox

x_1=1;

x_2=1;

h_1=1;

h_2=1;

h_3=1;
```

```
p_1=1;

p_2=1;

p_3=1;

theta_3=1;

theta_4=1;

k_p1=12.41; % spring coefficient at...

k_p2=12.41; % spring coefficient at...

k_p3=12.41; % spring coefficient at...

k_p4=12.41; % spring coefficient at...

B_p1=1; percentage damping coefficient at...

B_p2=1; % damping coefficient at...

B_p3=1; % damping coefficient at...

B_p4=1; % damping coefficient at...

J_1=140352.8; % mass moment of inertia of link __

J_2=1535304; % mass moment of inertia of rack/link BD

J_3=140352.8; % mass moment of inertia of link __

M_1=5112; % mass of rack ???

% Transform modulus

syms L5 t2 a

L2 = 7*12; % length of link AB

L1 = 12; % length of ground link AD

L3 = 70; % MAYBE length of link CD

eq1 = L2*sin(t2) == L5*sin(a);

eq2 = L2*cos(t2)-L5*cos(a) == L1;

sol = solve([eq1,eq2],[L5,a]);
```

```
L5 = (24*((tan(t2/2)^2 + 1)*(16*tan(t2/2)^2 + 9))^(1/2))/(tan(t2/2)^2 + 1);

a = 2*atan((((tan(t2/2)^2 + 1)*(16*tan(t2/2)^2 + 9))^(1/2) + 4*tan(t2/2)^2 - 3)/(7*tan(t2/2)));

rho = asin(L3/L5);

t4 = rho-a;

t2 = asin(L5/L2);

t3 = acos(L3/L5)-a;

r2 = diff(t2);

r3 = diff(t3);

r4 = diff(t4);

display(r2);

display(r3);

display(r4);

r_1=r2;

r_2=r2;

r_3=r3;

r_4=r4;

% State equations

T_1=-r_1*(k_p1*x_1+(B_p1*((r_1*h_1/J_1)-p_1/M_1)));

T_2=-r_2*(k_p2*x_2+(B_p2*((r_2*h_1/J_1)-p_2/M_1)));

T_3=-r_3*(k_p3*theta_3+(B_p3*((r_3*h_1/J_1)-h_2/J_2)));

T_4=-r_4*(k_p4*theta_4+(B_p4*((r_4*h_1/J_1)-h_3/J_3)));

hprime_1=T_0-T_1-T_2-T_3-T_4;

pprime_1=-k_p1*x_1+(B_p1*((r_1*h_1/J_1)-p_1/M_1));

pprime_2=-k_p2*x_2+(B_p2*((r_2*h_1/J_1)-p_2/M_1));

xprime_1=(r_1*h_1/J_1)-p_1/M_1;
```

```
xprime_2=(r_2*h_1/J_1)-p_2/M_1;

hprime_2=T_3/r_3;

hprime_3=T_4/r_4;

thetaprime_3=(r_3*h_1/J_1)-h_2/J_2;

thetaprime_4=(r_4*h_1/J_1)-h_3/J_3;

% Find v = f(t)

% alone x-axis

sym vx

vx=x_1;

f1= -M_1*diff(vx)-(B_p1*r_1*h_1/J_1)*vx==-B_p1*r_1*h_1/J_1;

laplace(f1,vx);

% alone y-axis

sym vy

vy=x_2;

f1= -M_1*diff(vy)-(B_p2*r_2*h_1/J_1)*vy==-B_p2*r_2*h_1/J_1;

laplace(f1,vy);

v=sqrt(vx^2+vy^2);
```

10.6. Calculations

10.6.1. Main Mechanism Acceleration Analysis

Known information

Defining θ 2 as a Range Variable

Link Lengths

Link 1 $d := .900$

Link 2 $a := 1.875$

Link 3 $b := .900$

LInk 4 $c := 1.875$

$\theta 2 := 0 \cdot deg , 9 \cdot deg .. 167 \cdot deg$

Angular Velocity of Link 2

$\omega_2 := 1$

Acceleration of Link 2

$\alpha_2 := 1$

Determining Constants for Θ 4

$$K01 := \frac{d}{a}$$

$$K2 := \frac{d}{c}$$

$$K3 := \frac{a^2 - b^2 + c^2 + d^2}{2 \cdot a \cdot c}$$

$$K01 = 0.48$$

$$K2 = 0.48$$

$$K3 = 1$$

$$A1(\theta 2) := cos(\theta 2) - K01 - K2\ cos(\theta 2) + K3$$

$$B(\theta 2) := -2 \cdot sin(\theta 2)$$

$$C1(\theta 2) := K01 - (K2 + 1) \cdot cos(\theta 2) + K3$$

Open Configuration

$$\theta 41(\theta 2) := 2 \cdot \left(atan2\left(2 \cdot A1(\theta 2), -B(\theta 2) - \sqrt{B(\theta 2)^2 - 4 \cdot A1(\theta 2) \cdot C1(\theta 2)}\right)\right)$$

$$\theta 41(\theta 2) = \boxed{\ldots} \cdot deg$$

Determining Constants for Θ 3

$$K4 := \frac{d}{b}$$

$$K5 := \frac{\left(c^2 - d^2 - a^2 - b^2\right)}{2 \cdot a \cdot c}$$

$$K4 = 1$$

$$K5 = -0.23$$

$$D(\theta 2) := cos(\theta 2) - K01 + K4 \cdot cos(\theta 2) + K5$$

$$E(\theta 2) := -2 \cdot sin(\theta 2)$$

$$F1(\theta 2) := K01 + (K4)\cdot cos(\theta 2) + K5$$

Open Configuration

$$\theta 31(\theta 2) := 2\cdot\left(atan2\left(2\cdot D(\theta 2), -E(\theta 2) - \sqrt{E(\theta 2)^2 + 4\cdot D(\theta 2)\cdot F1(\theta 2)}\right)\right)$$

$\theta 31(\theta 2) =$

$\boxed{\quad\ldots}\ \cdot deg$

Determining Angular Velocity for Links 3 and Links 4

Open Configuration

$$\omega 31(\theta 2) := \frac{a\cdot\omega_2\cdot sin(\theta 41(\theta 2) - \theta 2)}{b\cdot sin(\theta 31(\theta 2) - \theta 41(\theta 2))}$$

$\omega 31(\theta 2) =$

$\boxed{\quad\ldots}$

$$\omega 41(\theta 2) := \frac{a\cdot\omega_2\cdot sin(\theta 2 - \theta 31(\theta 2))}{b\cdot sin(\theta 41(\theta 2) - \theta 31(\theta 2))}$$

$\omega 41(\theta 2) =$

$\boxed{\quad\ldots}$

Angular Acceleration of links 3 and 4

$$A34(\theta 2) := c\cdot sin(\theta 41(\theta 2))$$

$$D34(\theta 2) := c\cdot cos(\theta 41(\theta 2))$$

$$B34(\theta 2) := b\cdot sin(\theta 31(\theta 2))$$

$$E34(\theta 2) := b\cdot cos(\theta 31(\theta 2))$$

$$A34(\theta2) = \boxed{\quad\ldots} \cdot deg$$

$$B34(\theta2) = \boxed{\quad\ldots} \cdot deg$$

$$D34(\theta2) = \boxed{\quad\ldots} \cdot deg$$

$$E34(\theta2) = \boxed{\quad\ldots} \cdot deg$$

$$C34(\theta2) := a \cdot \alpha_2 \cdot sin(\theta2) + a \cdot \left(\omega_2\right)^2 cos(\theta2) + b \cdot (\omega31(\theta2))^2 \cdot cos(\theta31(\theta2)) - c \cdot (\omega41(\theta2))^2 cos(\theta41(\theta2))$$

$$C34(\theta2) = \boxed{\quad\ldots}$$

$$F34(\theta2) := a \cdot \alpha_2 \cdot cos(\theta2) - a \cdot \left(\omega_2\right)^2 \cdot sin(\theta2) - b \cdot (\omega31(\theta2))^2 \cdot sin(\theta31(\theta2)) + c \cdot (\omega41(\theta2))^2 \cdot sin(\theta41(\theta2))$$

$$F34(\theta2) = \boxed{\quad\ldots}$$

Angular Acceleration of Link 31

$$\alpha 31(\theta 2) := \frac{C34(\theta 2)\cdot D34(\theta 2) - A34(\theta 2)\cdot F34(\theta 2)}{A34(\theta 2)\cdot E34(\theta 2) - B34(\theta 2)\cdot D34(\theta 2)}$$

$\alpha 31(\theta 2) =$

$\boxed{\quad ...}$

Angular Acceleration of Link 41

$$\alpha 41(\theta 2) := \frac{C34(\theta 2)\cdot E34(\theta 2) - B34(\theta 2)\cdot F34(\theta 2)}{A34(\theta 2)\cdot E34(\theta 2) - B34(\theta 2)\cdot D34(\theta 2)}$$

$\alpha 41(\theta 2) =$

$\boxed{\quad ...}$

Euler Identity Expansion for point A

$$AA = a\cdot\alpha_2\cdot\left(-sin\left(\theta_2\right) + j\cdot cos\left(\theta_2\right)\right) - a\cdot\left(\omega_2\right)^2\cdot\left(cos\left(\theta_2\right) + j\cdot sin\left(\theta_2\right)\right)$$

$$AAX(\theta 2) := \left[-a\cdot\alpha_2\cdot sin(\theta 2) - a\cdot\left(\omega_2\right)^2\cdot cos(\theta 2)\right]$$

$AAX(\theta 2) =$

$\boxed{\quad ...}$

$$AAY(\theta 2) := -a\cdot\alpha_2\cdot cos(\theta 2) - a\cdot\left(\omega_2\right)^2\cdot sin(\theta 2)$$

$AAY(\theta 2) =$

$\boxed{\quad ...}$

$$AA(\theta 2) := \sqrt{(AAX(\theta 2))^2 + (AAY(\theta 2))^2}$$

$$\theta AA(\theta 2) := atan2(AAX(\theta 2), AAY(\theta 2))$$

$AA(\theta 2) =$

$\boxed{\quad ...}$

$\theta AA(\theta 2) =$

$\boxed{\quad ...} \cdot deg$

Acceleration at point B

$$ABX(\theta 2) := c\cdot\left[-\alpha 41(\theta 2)\cdot sin(\theta 41(\theta 2)) - (\omega 41(\theta 2))^2\cdot cos(\theta 41(\theta 2))\right]$$

$ABX(\theta 2) =$

$\boxed{\quad ...}$

$$ABY(\theta 2) := c\cdot\left[\alpha 41(\theta 2)\cdot cos(\theta 41(\theta 2)) - (\omega 41(\theta 2))^2\cdot sin(\theta 41(\theta 2))\right]$$

$ABY(\theta 2) =$

$\boxed{\quad ...}$

$$AB(\theta 2) := \sqrt{(ABX(\theta 2))^2 + (ABY(\theta 2))^2}$$

$AB(\theta 2) =$

$\boxed{\quad ...}$

$$\theta AB(\theta 2) := atan2(ABX(\theta 2), ABY(\theta 2))$$

$\theta AB(\theta 2) =$

$\boxed{\quad ...} \cdot deg$

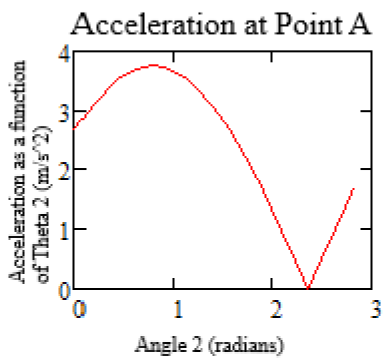

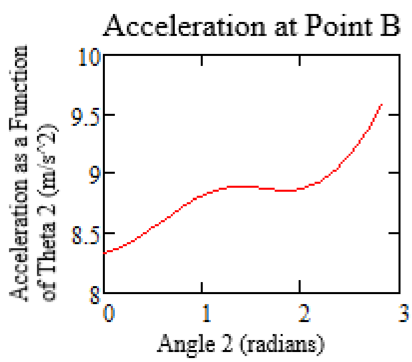

Virtual Work Method

$Ix := .333$

$Iy := .333$

$Ixy := .25$

$IG2 := Ixy$

$IG3 := Ixy$

$IG4 := Ixy$

$m2 := 1.568$

$m3 := 3.266$

$$m4 := 1.568$$

$$T12 := \frac{1}{\omega_2} \cdot \begin{bmatrix} m2 \cdot (aG2x \cdot vG2x + aG2y \cdot vG2y) + m3 \cdot (aG3x \cdot vG3x + aG3y \cdot vG3y) \ldots \\ + m4 \cdot (aG4x \cdot vG4x + aG4y \cdot vG4y) + (IG2 \cdot \alpha 2 \cdot \omega 2 + IG3 \cdot \alpha 31 \cdot \omega 31 + IG4 \cdot \alpha 41 \cdot \omega 41) \ldots \\ + -(FP3x \cdot vP3x + FP3y \cdot vP3y) - (FP4x \cdot vP4x + FP4y - vP4y) - T3 \cdot \omega 31 - T4 \cdot \omega 41 \end{bmatrix}$$

10.7.2 Driver Dyad Acceleration Analysis

Known information

Link 1 $d := .300$

Link 2 $a := .298$

Link 3 $b := .772$

LInk 4 $c := .300$

$$\theta_2 := 175 \cdot deg$$

$$\omega_2 := 1$$

$$\alpha_2 := 0$$

Determining Constants for Θ 4

$$K_1 := \frac{d}{a}$$

$$K_2 := \frac{d}{c}$$

$$K_3 := \frac{a^2 - b^2 + c^2 + d^2}{2 \cdot a \cdot c}$$

$$K_1 = 1.007$$

$$K_2 = 1$$

$$K_3 = -1.83$$

$$A := \cos(\theta_2) - K_1 - K_2 \cos(\theta_2) + K_3$$

$$A = -2.837$$

$$B := -2 \cdot \sin(\theta_2)$$

$$B = -0.174$$

$$C := K_1 - (K_2 + 1) \cdot \cos(\theta_2) + K_3$$

$$C = 1.169$$

Open Configuration

$$\theta_{41} := 2 \cdot \left(\operatorname{atan2}\left(2 \cdot A, -B - \sqrt{B^2 - 4 \cdot A \cdot C}\right)\right)$$

$$\theta_{41} = -297.064 \cdot \deg$$

Determining Constants for Θ 3

$$K_4 := \frac{d}{b}$$

$$K_5 := \frac{\left(c^2 - d^2 - a^2 - b^2\right)}{2 \cdot a \cdot c}$$

$$K_4 = 0.389$$

$$K_5 = -3.83$$

$$D := \cos\left(\theta_2\right) - K_1 + K_4 \cdot \left(\cos\left(\theta_2\right)\right) + K_5$$

$$D = -6.22$$

$$E := -2 \cdot \sin\left(\theta_2\right)$$

$$E = -0.174$$

$$F := K_1 + \left(K_4 - 1\right) \cdot \cos\left(\theta_2\right) + K_5$$

$$F = -2.214$$

Open Configuration

$$\theta_{31} := 2 \cdot \left(\operatorname{atan2}\left(2 \cdot D, -E - \sqrt{E^2 + 4 \cdot D \cdot F}\right)\right)$$

$$\theta_{31} = -299.534 \cdot \deg$$

Determining Angular Velocity

Open Configuration

$$\omega_{31} := \frac{a \cdot \omega_2 \cdot \sin\left(\theta_{41} - \theta_2\right)}{b \cdot \sin\left(\theta_{31} - \theta_{41}\right)}$$

$$\omega_{31} = 8.3$$

$$\omega_{41} := \frac{a \cdot \omega_2 \cdot \sin(\theta_2 - \theta_{31})}{b \cdot \sin(\theta_{41} - \theta_{31})}$$

$$\omega_{41} = 8.148$$

Angular Acceleration of links 3 and 4

$$A := c \cdot \sin(\theta_{41})$$

$$B := b \cdot \sin(\theta_{31})$$

$$D := c \cdot \cos(\theta_{41})$$

$$E := b \cdot \cos(\theta_{31})$$

$$A = 0.267$$

$$B = 0.672$$

$$D = 0.136$$

$$E = 0.381$$

$$C := a \cdot \alpha_2 \cdot \sin(\theta_2) + a \cdot (\omega_2)^2 \cos(\theta_2) + b \cdot (\omega_{31})^2 \cdot \cos(\theta_{31}) - c \cdot (\omega_{41})^2 \cos(\theta_{41})$$

$$C = 16.86$$

$$F := a \cdot \alpha_2 \cdot \cos(\theta_2) - a \cdot (\omega_2)^2 \cdot \sin(\theta_2) - b \cdot (\omega_{31})^2 \cdot \sin(\theta_{31}) + c \cdot (\omega_{41})^2 \cdot \sin(\theta_{41})$$

$$F = -28.568$$

$$\alpha_{31} := \frac{C \cdot D - A \cdot F}{A \cdot E - B \cdot D}$$

$$\alpha_{31} = 995.11$$

$$\alpha_{41} := \frac{C \cdot E - B \cdot F}{A \cdot E - B \cdot D}$$

$$\alpha_{41} = 2.565 \times 10^{3}$$

10.7. Bibliography

[1] M. Paine, “Bike Racks on the Front of Buses: Engineering and Road Safety Issues,” Oct. 1997.

[2] K. Upton, “Bigger bus racks for bikes? Maybe,” 2011. [Online]. Available: https://thesource.metro.net/2011/08/10/bigger-bus-racks-for-bikes-maybe/. [Accessed: 26-Sep-2019].

[3] “Overview of Transit Vehicles.”.

[4] R. Merzouki, A. K. Samantaray, P. M. Pathak, and B. O. Bouamama, “Intelligent Mechatronic Systems: Modeling, Control and Diagnosis,” 2012.

[5] B. I. GUIDE, “STATE TRANSIT.”.

[6] C. C. Gordon et al., “Anthropometric Survey of U.S. Army Personnel: Summary Statistics, Interim Report for 1988,” Mar. 1989.

[7] “Metals and Alloys - Densities,” 2004. [Online]. Available: https://www.engineeringtoolbox.com/metal-alloys-densities-d_50.html.

[8] J. T. Doolittle, Integration of bicycles and transit. United States, 1994.

[9] S. Bowers, “Bike fit variables: No. 3 wheelbase,” 11-Oct-2018. [Online]. Available: https://www.cyclist.co.uk/in-depth/5444/bike-fit-variables-no-3-wheelbase.

[10] D. K. Boyle, T. C. R. Program, T. R. Board, and N. A. of S. Medicine Engineering, and, “Better On-Street Bus Stops.” The National Academies Press, 2015, doi: 10.17226/22175.

[11] FireX, “How Much Do Bikes Weigh? The Importance of Bicycle Weight,” 28-Apr-2019. [Online]. Available: https://thexfire.com/bike-weighs.

[12] “Platform Length,” 2016. [Online]. Available: https://nacto.org/publication/transit-street-design-guide/stations-stops/stop-design-factors/platform-length/. [Accessed: 19-Feb-2020].

[13] S. N. Inc., “Transit Bike Racks,” 2019. [Online]. Available: https://www.sportworks.com/products/transit-bike-racks. [Accessed: 30-Sep-2019].

[14] T. Corfield, “MTB Geometry – The new Normal,” 13-Aug-2017. [Online]. Available: https://enduro-mtb.com/en/mtb-geometry-new-normal/.

[15] U. S. D. of T.-F. H. Administration, “Oversize/Overweight Load Permits,” 26-Jul-2019. [Online]. Available: https://ops.fhwa.dot.gov/freight/sw/permit_report/index.htm.